SOME OBSERVED SEASONAL CHANGES IN
EXTRATROPICAL GENERAL CIRCULATION:
A STUDY IN TERMS OF VORTICITY

BY

SRINIVASAN SRIVATSANGAM

Atmospheric Science
PAPER NO.

204

DEPARTMENT OF ATMOSPHERIC SCIENCE

COLORADO STATE UNIVERSITY

FORT COLLINS, COLORADO

BIBLIOGRAPHIC DATA SHEET	1. Report No. CSU-ATSP-204	2.	3. Recipient's Accession No.
4. Title and Subtitle Some Observed Seasonal Changes in Extratropical General Circulation: A Study in Terms of Vorticity			5. Report Date July, 1973
			6.
7. Author(s) SRINIVASAN SRIVATSANGAM			8. Performing Organization Rept. No. 204
9. Performing Organization Name and Address Dept. of Atmospheric Science, Colorado State University, Fort Collins, Colo. 80521			10. Project/XXXXXXXXXXXNo. 1989
			11. Contract/Grant No. NGR-06-002-098
12. Sponsoring Organization Name and Address National Aeronautics and Space Administration Washington, D.C.			13. Type of Report & Period Covered
			14.

15. Supplementary Notes

16. Abstracts

Analyses of relative geostrophic vorticity ζ_g show that the r.m.s. values of this parameter represent the normal state of the lower atmosphere in the extratropics. The zonal means of the temporal r.m.s. value of ζ_g -- called K -- are presented for four months and reveal the migration of Extratropical Frontal Jet Streams. The composition of the temporal r.m.s. vorticity maxima is also discussed.

17. Key Words and Document Analysis. XXXXXXXXXXX

    Seasonal Changes
    Extratropics
    General Circulation
    Vorticity

17b. Identifiers/Open-Ended Terms

17c. COSATI Field/Group

18. Availability Statement Release unlimited	19. Security Class (This Report) UNCLASSIFIED	21. No. of Pages 75
	20. Security Class (This Page) UNCLASSIFIED	22. Price

SOME OBSERVED SEASONAL CHANGES IN EXTRATROPICAL

GENERAL CIRCULATION: A STUDY IN TERMS

OF VORTICITY

by

Srinivasan Srivatsangam

Department of Atmospheric Science

Colorado State University

Fort Collins, Colorado

August, 1973

Atmospheric Science Paper No. 204

ℐℒ

ABSTRACT

Extratropical eddy distributions in four months typical of the four seasons are treated in terms of temporal mean and temporal r.m.s. values of the geostrophic relative vorticity. The geographical distributions of these parameters at the 300 mb level show that the arithmetic mean fields are highly biased representatives of the extratropical eddy distributions.

The zonal arithmetic means of these parameters are also presented. These show that the zonal-and-time mean relative vorticity is but a small fraction of the zonal mean of the temporal r.m.s. relative vorticity, K. The reasons for considering the r.m.s. values as the temporal normal values of vorticity in the extratropics are given in considerable detail.

The parameter K is shown to be of considerable importance in locating the Extratropical Frontal Jet Streams (EFJ) in time-and-zonal average distributions.

The study leads to an understanding of the seasonal migrations of the EFJ which have not been explored until now.

TABLE OF CONTENTS

Page

TABLE OF CONTENTS (cont'd)

iii

LIST OF TABLES

LIST OF FIGURES

1. Introduction

In an earlier paper (Srivatsangam, 1973; hereafter referred to as Paper A) the author presented the results of a study of the distribution of geostrophic relative vorticity in the Northern Hemisphere in Jan. 1970. There vorticity distribution was studied in terms of arithmetic means and root mean square values. The arithmetic zonal-and-time mean values were thereby shown to be but a small fraction of the normal vorticity of the atmosphere. The values of the parameter K given by

$$K = [\{\zeta_g\}_{(\lambda)}]_{(t)} \simeq [\{\zeta_g\}_{(t)}]_{(\lambda)} \tag{1}$$

(for an explanation of symbols please see Table 1) were considered to be the normal values of vorticity in the atmosphere, as opposed to the arithmetic zonal-and-time mean values which represent only the vorticity associated with the long-term zonal circulation, or the field of $[u]_{(t,\lambda)}$ (See, for example, Lorenz, 1967, p. 32.) Since the greater part of the vorticity associated with extratropical jet streams is in eddy form, the consideration of a 'normal' field of vorticity leads to a better understanding of the time-and-zonal mean locations and intensities of jet streams especially because of the great concentration of vorticity just below the tropopause. Above the jet-stream level the concentration of the K isopleths is much greater and helps in distinguishing between the troposphere and the stratosphere.

These encouraging results urged a study of the distribution of K in different seasons and resulted in this report.

Table 1

Definitions of Symbols

a	mean radius of the earth.
$f(x,...)$	mathematical function, not the Coriolis acceleration.
$f = 2 \Omega \sin \phi$	Coriolis acceleration.
H	geopotential height

$$K = [\{\zeta_g\}_{(\lambda)}]_{(t)} \simeq [\{\zeta_g\}_{(t)}]_{(\lambda)}$$
$$\simeq \{\zeta_g\}_{(t,\lambda)} \simeq \{\zeta_g\}_{(\lambda,t)}$$

r.h.s.	the right hand side of an Equ.
t	time.
u	zonal component of the observed wind.
u_g	zonal component of the geostrophic wind.
$\beta = \partial f/\partial(a\phi)$	the Rossby parameter.
ζ_g	relative geostrophic vorticity.
λ	longitude.
σ_x	the standard deviation of parameter x in some arbitrary independent variable k.
ϕ	latitude.
Ω	angular velocity of the earth.
$[f]_{(x)}$	the arithmetic mean of $f(x,...)$ in x.

$$[\,[f]_{(x)}\,]_{(y)} = [f]_{(x,y)}$$
$$(f)_{(x)} = f(x,...) - [f]_{(x)}$$

$\{f\}_{(x)}$	the root mean square value of $f(x,...)$ in x.

$$\{f\}_{(x,y)} \simeq \{f\}_{(y,x)}$$

$$([H]_{(t,\lambda)})_{(\phi)} = [H]_{(t,\lambda)} - [H]_{(t,\lambda,\phi)}$$

the deviation of zonally and temporally averaged geopotential height of an isobaric surface from the hemispheric time-mean value.

$|x|$ modulus of x

$< f (x,y) >$ matrix of f in x and y.

2. Data and Analytical Procedure

In this study the distributions of $[\zeta_g]_{(t,\lambda)}$, $[\{\zeta_g\}_{(\lambda)}]_{(t)}$, $[H]_{(t,\lambda)} - [H]_{(t,\lambda,\phi)}$ and the geographical distributions of $[\zeta_g]_{(t)}$ and $\{\zeta_g\}_{(t)}$ for the months July 1969, October 1969, January 1970 and April 1970 are presented and discussed. The data for the study was the daily geopotential height distributions of the 700; 500; 400; 300; 200 and 100 mb surfaces as obtained from the National Meteorological Center (NMC) data tapes. All months except October 1969 had missing data for a few days. But for every month studied here we had more than 20 days of data. Thus the values presented here must be reasonably representative of monthly averages obtained by including all data. This is not equivalent to stating that the results presented here are true climatological averages. This is certainly not the case. Some deviations of these results from long-period averages will be discussed in later sections of this report.

The analysis for the four months was carried out by Mrs. Alice Fields. The CDC 6400 computer at the Colorado State University was used for all calculations. While the daily geopotential height data were being converted to geostrophic relative vorticity and put on tapes the zonal r.m.s. values of ζ_g were calculated thus providing us with data for checking the equivalence of the parameters in Equ. 1. Initially the geographical distributions were hand analyzed. But later analyses were carried out by the computer.

3. Averaging Conventions

These were discussed in detail in Paper A, and are summarized in Table 1. The averaging conventions followed here are those due to Reiter (1969a; 1969b, p. 6-8) and Srivatsangam (Paper A) . As discussed in Paper A, in general

$$[\{\zeta_g\}_{(t)}]_{(\lambda)} \neq [\{\zeta_g\}_{(\lambda)}]_{(t)} \tag{2}$$

since the $<|\zeta_g(\lambda,t)|>$ matrices are non-square and do not have identical values for each matrix element. But apparently the $|\zeta_g(t,\lambda)|$ values are sufficiently homogeneous so that the inequality sign in Equ. (2) above may be replaced by an "equal" sign. This was shown to be the case for Jan. 1970 in Paper A. In the present paper we present the values for the other three months of $[\{\zeta_g\}_{(t)}]_{(\lambda)}$ and $[\{\zeta_g\}_{(\lambda)}]_{(t)}$ in Appendices 1, 1a and 1b. From these data it is seen readily that for each of the month considered the approximation of Equ. 1 holds.

4. The Distribution of $[\zeta_g]_{(t,\lambda)}$

In Figures 1a to 1d the distribution of $[\zeta_g]_{(t,\lambda)}$ during each of the 4 months considered is presented. There is considerable similarity between the distributions of July, October and April, especially in the middle latitudes (40N to 60N). In these latitudes mild cyclonic conditions $(\zeta_g \simeq 1 \times 10^{-5} s^{-1}$ at the jet-stream level) prevail. In the subpolar latitudes (60N to 75N) cyclonic velocity of smaller magnitude prevails in October and April, and anticyclonic mean conditions are obtained only in July. The major difference between these 3 months is the July intensification and northward displacement of the subtropical high pressure systems. The movement is seen to be some 10 Deg. latitude northward. The intensity nearly doubles in the 200 mb-300 mb layer. From Appendices 3 and 4 it might be seen that the intensity of the subtropical high pressure systems at 25N, 200 mb in January exceeds the July maximum at 200 mb at 35N. The January distribution of $[\zeta_g]_{(t,\lambda)}$ is also of interest because of the occurrence of the absolute maximum of $[\zeta_g]_{(t,\lambda)}$ among all the 4 months considered. This

is located at the level of the Subtropical Jet Stream (200 mb) but to the north of the STJ axis, which is at about 27N (see Krishnamurti, 1961). The poleward displacement of the $[\zeta_g]_{(t,\lambda)}$ maximum relative to the STJ axis is due to the fact that the isotach maxima imbedded in the STJ are some 5 to 10 deg. latitude poleward of the STJ axis (see Krishnamurti, op. cit.)

Since the distribution of $[\zeta_g]_{(t,\lambda)}$ represents the vorticity distribution due to the zonally and temporally averaged zonal geostrophic motion or $[u_g]_{(t,\lambda)}$ this field offers a valuable check into our calculations. $[u_g]_{(t,\lambda)}$ is readily computed from the $[H]_{(t,\lambda)}$ field by the geostrophic relationship:

$$[u_g]_{(t,\lambda)} = \frac{1}{f} \frac{\partial}{\partial y} [H]_{(t,\lambda)} \tag{3}$$

The values of $[H]_{(t,\lambda)}$ for the 4 months considered here are presented in Appendix 2. From these the geostrophic wind and geostrophic relative vorticity were computed, the latter from the expression

$$[\zeta_g]_{(t,\lambda)} = \frac{\tan \phi}{af} \frac{\partial}{\partial y} [H]_{(t,\lambda)} - \frac{1}{f} \frac{\partial^2}{\partial y^2} [H]_{(t,\lambda)}$$

$$+ \frac{\beta}{f^2} \frac{\partial}{\partial y} [H]_{(t,\lambda)} \tag{4}$$

and are presented in Appendices 3 and 4 respectively. It might be seen that Equ. 4 includes both the meridional shear of $[u]_{(t,\lambda)}$ and the effect of the convergence of meridians on $[u]_{(t,\lambda)}$. A comparison of the values of $[\zeta_g]_{(t,\lambda)}$ in Appendix 4 and the values in Figures 1a to 1d shows that the two are quite comparable.

In order to check the correctness of our results further and to compare the properties of the circulation systems of the 1969-1970 period with those

of more truly climatic averages, the 5-year mean geopotential height data

presented by Oort and Rasmusson (1971, p. 84) were converted into

$[u_g]_{(t,\lambda)}$ and $[\zeta_g]_{(t,\lambda)}$ values and presented as Appendices 5 and 6

respectively. Oort and Rasmusson did not present such computed results

except for $[u_g]_{(t,\lambda)}$ at the 200 mb level (Oort and Rasmusson, 1971,

p. 18).

A comparison of $[u_g]_{(t,\lambda)}$ in Appendices 3 and 5 shows that the monthly

means for 1969-70 did not differ very much from the 5-year means, except

in January. The maxima in July, October and April are in good agreement

with regard to magnitude. In July 1969 the maximum is at 42.5N and has

a value of 22.6 ms^{-1}; the corresponding values for the 5-year period are

42.5N and 21.8 ms^{-1}. In October 1969 the maximum is at 42.5N and has a

value of 27.7 ms^{-1}; the corresponding values for the 5-year period are 37.5N

and 28.6 ms^{-1}, indicating a northward displacement of the maximum in 1969.

In January and April the maxima of $[u_g]_{(t,\lambda)}$ are spread out latitudi-

nally. (This is also true of October.) Table 2 gives the magnitudes.

and the latitudes of occurrence of maxima for these two months from which

it is seen that the April 1970 maximum was relatively more spread-out and

that the January 1970 maximum had a higher value than the 5-year data

maximum, the excess being some 6 ms^{-1} at 32.5N. This excess is probably

due to the anomalies of the geopotential height fields in January 1970 which

amounted to -100m and -170m over the Pacific and Atlantic Oceans respectively,

at the 700 mb level. (For further discussion see Paper A.)

It should be mentioned here that the geostrophic zonal wind is generally

an overestimate of the true zonal wind in the zones of strong westerly

winds. This is due to the fact that the geostrophic wind is a non-accelerated

wind whereas zonal winds with trajectories similar to latitude circles must

be decelerated, and this is approximately true of winds in the vicinity of

the STJ (see Lorenz, 1967, p. 33). Hence in general

$$[u]_{(t,\lambda)} < [u_g]_{(t,\lambda)} \tag{5}$$

(see also Oort and Rasmusson, 1971, p. 17-18).

The effect of this on the relationship between $[\zeta]_{(t,\lambda)}$ and $[\zeta_g]_{(t,\lambda)}$

could not be studied for the 1969-70 period since we were not computing

$[u]_{(t,\lambda)}$. But a check was possible through the Oort and Rasmusson (op. cit.)

data.

In Appendix 7 we present the values of $[\zeta]_{(t,\lambda)}$ obtained from the

$[u]_{(t,\lambda)}$ data of Oort and Rasmusson (1971, p. 76-77). A comparison of

these values with the $[\zeta_g]_{(t,\lambda)}$ values for the same period (see Appendix 6)

shows that the geostrophic vorticity is an overestimate of the vorticity

associated with the observed zonal wind. Thus, in general

$$|[\zeta]_{(t,\lambda)}| < |[\zeta_g]_{(t,\lambda)}| \tag{6}$$

Hence the values of the different vorticity parameters presented in this

paper must all be considered to be slight overestimates of the observed

values. (See also Reiter 1963, p. 18.)

A consideration of the $[\zeta_g]_{(t,\lambda)}$ distributions of Appendices 4 and 6

shows that the magnitudes of $[\zeta_g]_{(t,\lambda)}$ in the period 1969-70 were comparable

to the mean vorticity in the 5-year period analyzed by Oort and Rasmusson.

The ratio of our data to the Oort and Rasmusson data at the 200 mb level at 40N

in January - where the annual maximum of $[\zeta_g]_{(t,\lambda)}$ occurs - is approximately

11:9 which is comparable to the ratio of the $[u_g]_{(t,\lambda)}$ maxima which is 10:9.

Table 2

The Magnitudes and Latitudes of Occurrence of
$[u_g]_{(t,\lambda)}$ Maxima in January and April
Units: ms^{-1}

LAT. DEG. NORTH	JAN		APR	
	ORa	SRI	ORa	SRI
27.5	45.3	48.1	33.3	30.8
32.5	44.8	50.9	34.2	33.5
37.5				31.0

NB: ORa stands for Oort and Rasmusson (1971).
SRI stands for the present report.
All maxima are at the 200 mb level.

5. The Distribution of Mass or $[H]_{(t,\lambda)} - [H]_{(t,\lambda,\phi)}$

Because of the inter-relationship between the distribution of $[H]_{(t,\lambda)} - [H]_{(t,\lambda,\phi)}$ and the field of $[u_g]_{(t,\lambda)}$ (see Equ. 3) the former is of considerable meteorological interest. Although the literature abounds with statistics of the latter parameter (see, for example, Lorenz, 1967, p. 32-39) the related distribution of mass has never been presented in the form $[H]_{(t,\lambda)} - [H]_{(t,\lambda,\phi)}$, as far as the author knows. This might be due to the difficulty in establishing an acceptable value of $[H]_{(t,\lambda,\phi)}$. The difficulty arises because of the observed fact that the thermal equator of our planet does not coincide with its geographical equator. The thermal equator is a surface which has considerable variability in the ϕ,λ,t coordinates and also to a lesser extent in p over a belt of (ϕ,λ,t). Thus the true value of $[H]_{(t,\lambda,\phi)}$ which could only be obtained by averaging the values of (t,λ,ϕ,p) in a "meteorological hemisphere," i.e., a hemisphere defined with respect to the meteorological equator, becomes a considerable task. If the value of $[H]_{(t,\lambda,\phi)}$ were not exact, the zero isopleth of the $[H]_{(t,\lambda)} - [H]_{(t,\lambda,\phi)}$ distribution will be misplaced and so also all the other isopleths.

On the other hand the $[u_g]_{(t,\lambda)}$ distribution depends only upon the local geopotential height gradients measured over isobaric surfaces, and does not involve assumptions about the mean mass field.

Despite all these considerations the author chooses to present the mean mass fields for the different months considered in Figures 2a to 2d. Here the value of $[H]_{(t,\lambda,\phi)}$ has been assumed to be $[H]_{(t,\lambda)}$ arithmetically averaged over the latitudinal belt equator to 80N. The magnitudes of the isopleths in these diagrams could not be given much significance in view of the above considerations, especially in July when the meteorological equator is

well into the northern hemisphere continents. However, Figures 2b to 2d are probably representative of the actual mean mass distribution in the northern "meteorological hemisphere" because the meteorological equator is southward of the geographical equator, thus equalizing the effects of lack of data north of 80N.

The relative concentration of the isopleths of $[H]_{(t,\lambda)}$ - $[H]_{(t,\lambda,\phi)}$ in a zonal belt is an indicator of the intensity of $[u_g]_{(t,\lambda)}$ in that belt. Comparisons of Figures 2a to 2d and the tabulated values of $[u_g]_{(t,\lambda)}$ for the corresponding months in Appendix 3 reveals the mutual agreement of the data.

6. Some Properties of $\{\zeta_g\}_{(t)}$ and K

Some of the mathematical properties of the parameter K which is defined through Equ. 1 have been discussed in Section 3 above. Several of the meteorological properties and uses of K were described in Paper A. Here we shall treat the mathematics of the process of taking root mean square values of meteorological quantities and consider their implications to the general circulation of the atmosphere.

First of all, we shall consider some of the fundamental reasons under-lying this study.

The distinguishing feature of the root mean square averaging procedure as applied to an inhomogeneous array of positive and negative numbers is that the signs of the numbers are not taken into account but only the magnitudes. The vorticity of extratropical eddies might be considered as constituting such an array (in time) at each different location (ϕ,λ,p). The temporal arithmetic average of such an array enables us to quantitatively state the mean cyclonic vorticity or anticyclonic vorticity of these locations.

These mean quantities could be further averaged with respect to meridians to obtain zonal-and-time averages, such as are presented in Figures 1a to 1d; these then represent the temporal mean cyclonic vorticity and anticyclonic vorticity of the different latitudes or zonal belts.

These mean values have considerable significance if the array is reasonably homogeneous, i.e., if the fluctuations from the mean state are of small magnitudes. Symbolically, any meteorological parameter -- and here we shall consider geostrophic relative vorticity -- could be represented at each location (t,λ,ϕ,p) by

$$\zeta_g = [\zeta_g]_{(t)} + (\zeta_g)_{(t)}$$

$$= \underset{a}{[\zeta_g]_{(t,\lambda)}} + \underset{b}{([\zeta_g]_{(t)})_{(\lambda)}} + \underset{c}{[(\zeta_g)_{(t)}]_{(\lambda)}}$$

$$+ \underset{d}{(\zeta_g)_{(t,\lambda)}} \tag{7}$$

Here term a represents the vorticity of the zone-and-time averaged zonal geostrophic wind, or, in Lorenz's (1967, p. 32) terminology the vorticity of the long-term (geostrophic) zonal circulation; term b represents the vorticity of the standing eddies; term c that of the transient zonal circulations; and term d the vorticity of the transient eddies.

Let us consider the effect of arithmetic averaging on these four terms. Taking the temporal mean first,

$$[\zeta_g]_{(t)} = \underset{a}{[\zeta_g]_{(t,\lambda)}} + \underset{b}{([\zeta_g]_{(t)})_{(\lambda)}} \tag{8}$$

Here the second average with respect to time is omitted on the right hand side since it is not necessary, being already included in the two terms. From Equ. 8 we see that the time averaging has eliminated the

transient eddies and the transient zonal circulations. Let us consider regions of the globe where

$$|c| + |d| >> |a| + |b| \qquad (9)$$

where the letters denote the terms in Equ. 7. Then maps of $[\zeta_g]_{(t)}$ are not good representatives of the normal weather conditions of these locations, as might be seen from Equ. 8.

The arithmetic averaging of Equ. 8 with respect to meridians leads to

$$[\zeta_g]_{(t,\lambda)} = [\zeta_g]_{\underset{a}{(t,\lambda)}} .$$

Thus the distribution of $[\zeta_g]_{(t,\lambda)}$ would not represent normal meteorological conditions fairly if

or,

$$\left.\begin{array}{c} |b| + |c| + |d| >> |a| \\[2mm] \left|([\zeta_g]_{(t)})_{(\lambda)}\right| + \left|[(\zeta_g)_{(t)}]_{(\lambda)}\right| + \left|(\zeta_g)_{(t,\lambda)}\right| \\[2mm] >> \left|[\zeta_g]_{(t,\lambda)}\right| \end{array}\right\} \qquad (10)$$

Inequality (10) is quite valid in the extratropics where the observed synoptic state is usually a disturbed state, and leads to an inequality such as (22) below.

Eddies are of very considerable importance in the extratropics. In fact neither the climate nor the weather of the extratropics could be understood without accounting for the eddies.

One way to study these eddy phenomena is to study the variances of the observed wind, temperature and other fields as is done in the extensive literature on the subject of available potential energy (see, for example,

Lorenz, 1967, and Reiter 1969b, for complete lists of references).
However, there is a need to represent the normal state of the extratropical
atmospheric circulation systems in time and time-and-longitude averaged
distributions (see Paper A).

The distributions of $\{\zeta_g\}_{(t)}$ and of K will be shown to filfill this
need.

From Equ. 7, ζ_g^2 could be obtained in the following form by simple
algebraic expansion:

$$\zeta_g^2 = \left[[\zeta_g]_{(t,\lambda)} + ([\zeta_g]_{(t)})_{(\lambda)} \right]^2$$

$$+ \left[([\zeta_g]_{(\lambda)})_{(t)} + (\zeta_g)_{(t,\lambda)} \right]^2$$

$$+ 2 \left[[\zeta_g]_{(t,\lambda)} + ([\zeta_g]_{(t)})_{(\lambda)} \right] \left[([\zeta_g]_{(\lambda)})_{(t)} + (\zeta_g)_{(t,\lambda)} \right] \qquad (11)$$

Here and in what follows the heavy square brackets do not have any significance
in averaging. Equ. 11 could be further expanded to give:

$$\zeta_g^2 = \underset{I}{[\zeta_g]^2_{(t,\lambda)}} + \underset{II}{([\zeta_g]_{(t)})^2_{(\lambda)}}$$

$$+ \underset{III}{([\zeta_g]_{(\lambda)})^2_{(t)}} + \underset{IV}{(\zeta_g)^2_{(t,\lambda)}}$$

$$+ \underset{V}{2[\zeta_g]_{(t,\lambda)}([\zeta_g]_{(t)})_{(\lambda)}} + \underset{VI}{2\,([\zeta_g]_{(\lambda)})_{(t)}(\zeta_g)_{(t,\lambda)}}$$

$$+ \underset{VII}{2[\zeta_g]_{(t,\lambda)}([\zeta_g]_{(\lambda)})_{(t)}} + \underset{VIII}{2\,[\zeta_g]_{(t,\lambda)}(\zeta_g)_{(t,\lambda)}}$$

$$+ \underset{IX}{2([\zeta_g]_{(t)})_{(\lambda)}([\zeta_g]_{(\lambda)})_{(t)}} + \underset{X}{2([\zeta_g]_{(t)})_{(\lambda)}(\zeta_g)_{(t,\lambda)}} \qquad (12)$$

In Equ. 12 term I is merely the square of the vorticity of the longterm zonal circulation; terms II, III and IV represent the variances of the vorticity due to standing eddies, transient zonal circulations and transient eddies, respectively. The other six terms represent the correlations between the terms a, b, c and d of Equ. 7. Term V represents the correlation between the vorticity of the longterm zonal circulation and of the standing eddies; term VI represents the correlation between transient zonal circulations and transient eddies. It might be noted that in time-averaging ζ_g^2 these terms will not disappear, there being no reason to assume *a priori* that transient zonal circulations and transient eddies are totally uncorrelated. However, terms VII to X will all disappear in time-averaging because each of these is the product of one transient and one non-transient component. Hence:

$$[\zeta_g^2]_{(t)} = [[\zeta_g]^2_{(t,\lambda)}]_{(t)} + [([\zeta_g]_{(t)})^2_{(\lambda)}]_{(t)}$$

$$+ [([\zeta_g]_{(\lambda)})^2_{(t)}]_{(t)} + [(\zeta_g)^2_{(t,\lambda)}]_{(t)}$$

$$+ 2[[\zeta_g]_{(t,\lambda)} ([\zeta_g]_{(t)})_{(\lambda)}]_{(t)}$$

$$+ 2[([\zeta_g]_{(\lambda)})_{(t)} (\zeta_g)_{(t,\lambda)}]_{(t)} \qquad (13)$$

Further averaging of Equ. 13 with respect to meridians eliminates the 5th and 6th right hand side terms because both of these terms involve one component which is a departure from the zonal average. Hence:

$$[[\zeta_g^2]_{(t)}]_{(\lambda)} = [\{\zeta_g\}^2_{(t)}]_{(\lambda)}$$

$$= [[\zeta_g]^2_{(t,\lambda)}]_{(t,\lambda)} + [([\zeta_g]_{(t)})^2_{(\lambda)}]_{(t,\lambda)}$$

$$+ [([\zeta_g]_{(\lambda)})^2_{(t)}]_{(t,\lambda)} + [(\zeta_g)^2_{(t,\lambda)}]_{(t,\lambda)} \qquad (14)$$

It is immediately seen that Equ. 14 is just an expanded meteorological form of the well-known statistical equation:

$$\sigma_x^2 = \overline{x^2} - \overline{x}^2$$

or,

$$\overline{x^2} = \overline{x}^2 + \sigma_x^2 \qquad (15)$$

where σ_x is the standard deviation of the parameter x in some independent variable k with respect to which arithmetic averaging (denoted by —) is done.

In order to obtain mathematical expressions for the parameters used in this report we take the square-root of Equ. 13. Hence:

$$\{\zeta_g\}_{(t)} = \left[[[\zeta_g]^2_{(t,\lambda)}]_{(t)} + [([\zeta_g]_{(t)})^2_{(\lambda)}]_{(t)} \right.$$

$$+ [([\zeta_g]_{(\lambda)})^2_{(t)}]_{(t)} + [(\zeta_g)^2_{(t,\lambda)}]_{(t)}$$

$$+ 2[[\zeta_g]_{(t,\lambda)}([\zeta_g]_{(t)})_{(\lambda)}]_{(t)}$$

$$\left. + 2[([\zeta_g]_{(\lambda)})_{(t)}(\zeta_g)_{(t,\lambda)}]_{(t)} \right]^{1/2} \qquad (16)$$

Thus the $\{\zeta_g\}_{(t)}$ values are seen to contain the correlation between the vorticity of the longterm zonal circulation and of the standing eddies, that between the vorticity of the transient zonal circulations and of the transient eddies (the 5th and 6th r.h.s. terms in Equ. 16) as well as the variances of the deviations from the vorticity of the longterm circulation

(the 2nd, 3rd and 4th r.h.s. terms of Equ. 16) and the square of the
vorticity of the longterm zonal circulation (the 1st r.h.s. term of
Equ. 16).

In order to study the importance of the correlation terms of Equ.
16, for which a qualitative explanation does not seem to exist at the
present time as far as the author knows, an expression for the zonal
r.m.s. value of $\{\zeta_g\}_{(t)}$ was obtained. This is given by

$$\{\{\zeta_g\}_{(t)}\}_{(\lambda)} = \left[\left[[\zeta_g]^2_{(t,\lambda)} \right]_{(t,\lambda)} + \left[([\zeta_g]_{(t)})^2_{(\lambda)} \right]_{(t,\lambda)} \right.$$
$$\left. + \left[([\zeta_g]_{(\lambda)})^2_{(t)} \right]_{(t,\lambda)} + \left[(\zeta_g)^2_{(t,\lambda)} \right]_{(t,\lambda)} \right]^{1/2} \qquad (17)$$

The 5th and 6th r.h.s. terms of Equ. 16 drop out in zonal averaging
because each involves one component which is a deviation from the zonal
mean.

A comparison of Equ. 17 with Equ. 14 shows that

$$\{\{\zeta_g\}_{(t)}\}_{(\lambda)} = [\{\zeta_g\}_{(t)}^2]^{1/2}_{(\lambda)} \qquad (18)$$

which serves as a check for the correctness of our previous equations.

In Appendices 8 and 9 we present the values of $\{\{\zeta_g\}_{(t)}\}_{(\lambda)}$ for
October 1969 and of $\{\{\zeta_g\}_{(\lambda)}\}_{(t)}$ for all the months considered. A
comparison of these values with one another and with the tabulated results
of Appendices 1a, 1b and 1c shows that the parameter K is given by

$$K = [\{\zeta_g\}_{(\lambda)}]_{(t)} \simeq [\{\zeta_g\}_{(t)}]_{(\lambda)}$$
$$\simeq \{\zeta_g\}_{(t,\lambda)} \qquad (19)$$

whereby it is denoted that

$$\{\zeta_g\}_{(t,\lambda)} = \{\{\zeta_g\}_{(t)}\}_{(\lambda)} \cong \{\{\zeta_g\}_{(\lambda)}\}_{(t)}$$

$$= \{\zeta_g\}_{(\lambda,t)} \qquad (20)$$

Since the values of $\{\zeta_g\}_{(t,\lambda)}$ do not include the effects of any correlation terms, whereas those of $[\{\zeta_g\}_{(t)}]_{(\lambda)}$ do include these, the results of comparing Appendices 1a, 1b, 1c, 8 and 9 are quite encouraging and reveal that correlations such as those represented by the 5th and 6th r.h.s. terms of Equ. 16 are not very important. Hence $\{\zeta_g\}_{(t)}$ could be approximated as follows:

$$\{\zeta_g\}_{(t)} \cong \left[[[\zeta_g]^2_{(t,\lambda)}]_{(t)} + [([\zeta_g]_{(t)})^2_{(\lambda)}]_{(t)} \right.$$

$$\left. + [([\zeta_g]_{(\lambda)})^2_{(t)}]_{(t)} + [(\zeta_g)^2_{(t,\lambda)}]_{(t)} \right]^{1/2} \qquad (21)$$

Thus for all practical purposes $\{\zeta_g\}_{(t)}$ and the parameter K both contain only the square-roots of the squared vorticity of the longterm zonal circulation and the variances of the vorticity deviations from the mean state. Thus they represent the summed (vorticity) effects of the longterm zonal circulation and the deviations from it.

The above equations and remarks show that the parameter K. and $\{\zeta_g\}_{(t)}$ are indeed representatives of the normal state of the atmosphere, especially when inequalities (9) and/or (10) are valid.

Some results obtained by applying these parameters to the geopotential height data of the extratropics of the Northern Hemisphere will be discussed below.

7. The Distributions of K

7A. Properties of the K maxima

We present the distributions of K in the four months considered in Figures 3a to 3d. A comparison of these with the distributions of $[\zeta_g]_{(t,\lambda)}$ in Figures 1a to 1d shows that with the exception of January the values of $[\zeta_g]_{(t,\lambda)}$ and K in each month could be related by

$$\left| [\zeta_g]_{(t,\lambda)} \right| << K \tag{22}$$

Hence the time-and-longitude average of the moduli of eddy vorticity is much greater than the vorticity of the $[u_g]_{(t,\lambda)}$ distribution in the troposphere and the lower stratosphere.

As was discussed in Paper A we find the densities of the K isopleths to be considerably different in the stratosphere and the troposphere. Thus a stratosphere which extends downward in the poleward direction is revealed in each month.

The maxima of K must occur at those levels where the isotach maxima imbedded in jet streams occur most frequently and/or with the largest magnitudes. These are also latitude belts in which the tropopause break will occur most frequently (see Paper A). From the studies of the transport of stratospheric radioactive debris into the troposphere (Reiter et al., 1967; Mahlman, 1967; and others) it is known that most of this transport is accomplished in regions of tropopause-break associated with lower tropospheric fronts. Hence the latitude belts of occurrence of K maxima are in general the regions most actively receiving stratospheric radio-active debris. An exception to this is the January maximum, which occurs in conjunction with the isotach maxima in the STJ-PFJ confluence regions

(see Paper A). Since the STJ does not have a baroclinic or frontal zone extending into the lower troposphere (see, for example, Reiter and Whitney, 1969) the southern part of the K maximum in January does not represent an important region for the radioactive debris transport into the lower troposphere. However, the partitioning of this maximum is difficult because of the day-to-day variability of jet stream location (see Reiter and Whitney, op. cit.)

The author wishes to re-emphasize here the possible significant anomalies of K in the period (1969-70) studied. Such anomalies would make the locations of K maxima given in Figures 3a to 3d non-typical. For true climatological location of these several more years of data would have to be studied. Even then great difficulties in the fore-casting of debris transfer will remain because of seasonal anomalies and intra-monthly variability. (For a detailed discussion of the stratospheric-tropospheric exchange processes see Reiter 1972, p. 61 to 102).

7B. The seasonal changes and migrations of extratropical jet streams

The distributions of K in the four months studied enable us to locate the time-and-zonal average positions of the extratropical jet streams approximately.

A comparison of Figures 3a to 3d shows that there is considerable similarity in the distribution of K in the mid-troposphere in all the four months. At the 700 mb level the maximum value of K is reached in January ($K = 2.5 \times 10^{-5} s^{-1}$). But in the other 3 months, at this level, the values of K are not much smaller ($K = 2 \times 10^{-5} s^{-1}$).

But as the altitude increases the pattern of K changes from month to month.

The upper tropospheric distributions of K in July and October have considerable similarity, the maxima of K constituting a single unbroken "roll" from 25N to 75N in each month.

Similarly the upper tropospheric distributions of K in January and April have much similarity. In both these months the maxima of K are bifurcated and exhibit distinct relative minima somewhere in the extratropics.

In JULY the maximum isopleths of K at jet-stream level have the smallest magnitudes of any month studied here. The highest isopleth in Figure 3a $(4.25 \times 10^{-5} s^{-1})$ is quite well spread-out across latitude circles, extending from approximately 38N to 55N. Another feature of the K maximum in this month is the higher altitude at which it occurs compared to the maximum, for example, of October. The Extratropical Frontal Jet Streams of January, April and October have the maximum K isopleth at approximately the 300 mb level and only lower value contours extend to the 250 mb or 200 mb level. Thus the maximum value of K in July occurs at higher altitudes than the maxima (associated with the EFJ) of the other three months. The reason for this must be the poleward migration of the subtropical high pressure systems in summer (see Fig. 2a). This migration tends to raise the tropopause in the midlatitudes in summer. Figure 3 e, which is an analysis of the radiosonde data of some coastal North American stations for July 1969, is presented in support of this state-ment. (Here the tropopause has been defined to be any isothermal or inversion layer 10 mb or more thick that occurs above the 400 mb level.) More extensive analyses of tropopause heights might be found in the U. S. Dept. of Commerce Daily Aerological Cross Sections (1962-63). The basic reasons for this raising of tropopause heights in summer are

the weakening of the pole to equator temperature gradient and the
relative increase of small-scale (Cb) convection in summer (see Gray,
1972).

The change in the maximum observed magnitude of K from July to
OCTOBER is as striking as the change in the geographical distribution
of $\{\zeta_g\}_{(t)}$ over this period (see Section 8). From an observed minimum
in July, the maximum of K rises in October to an absolute maximum of
any month studied here: The highest contour drawn in Figure 3b has a
value of $5.25 \times 10^{-5} s^{-1}$. This very large value of K which occurs in
conjunction with the PFJ is due to the common occurrence of low
index type patterns of circulation at the 300 mb level almost every
in this month. This leads to the simultaneous occurrence of large shears
and large curvatures of streamlines resulting in the very high values
of vorticity observed; during the other three months studied large
shears were generally observed when the flow was quasi-zonal. In
support of these observations we present Figures 6, 7 and 8 which are
the geopotential height distributions of the 300 mb surface on Oct. 17,
1969; Oct. 30, 1969; and Apr. 2, 1970 respectively. An example for
January 1970 has already been presented in Paper A.

The distribution of K in JANUARY 1970 is presented in Figure 3c.
This distribution has already been discussed in detail in Paper A, and
the reader is referred to it. The important feature of this diagram
is the definite bifurcation of K in the upper troposphere with a maximum
in the midlatitudes (approximately 30N to 50N) and another in the subpolar
latitudes (60N to 70N) with a relative minimum at 55N. These maxima
display the expected characteristics of the STF combined with the PFJ, and
AFJ. The maximum value of K in the subtropics (28N to 35N) occurs

at a lower pressure (approximately 200 mb) than the maximum at 40N,
which occurs in conjunction with the PFJ at a higher pressure (300 mb).
The upward slope of the K isopleths in the equatorward direction in
these latitudes in the troposphere is quite significant. From these
observations we could infer the following:

1) The midlatitude (30N to 50N) maximum of K in January is largely
due to the confluence regions of the STJ and the PFJ (see Krishnamurti,
1961).

2) The K maximum associated with the STJ is confined largely to
the upper troposphere whereas the maximum associated with the PFJ extends
downward considerably, because of the horizontal wind shears in the
polar frontal zone.

3) The time-and-zonal average position of the STJ is at a higher
level than that of the PFJ, as is the case with daily meridional
cross-sections.

The location of the secondary maximum of K in the subpolar latitudes,
which is due to the Arctic Front Jet Stream (see Paper A), leads to a
fourth observation:

4) The Arctic Front Jet Stream occurs at a lower altitude than
both the STJ and the PFJ. The K maximum associated with this jet stream
also extends downward, thus indicating the similarity between the AFJ
and the PFJ.

5) Since the maxima of K must occur in zonal belts where the
highest wind speeds are most frequently observed[*], these are also

---

[*] That this would lead to the maxima of K is seen from the
definition of jet streams: "(A jet stream) is a strong, narrow current,
concentrated along a quasi-horizontal axis in the upper troposphere or
in the stratosphere, characterized by strong vertical and lateral wind
shears..." (WMO, Res. 25 [EC-IX]).

zonal belts in which the phenomenon of tropopause break or folding will be observed most frequently (see Paper A).

Combining observations 3, 4 and 5 we could state the following:

6) Tropopause breaks must in general occur at increasingly lower altitudes (or higher pressures) in the poleward direction. Thus the tropopause itself slopes downward in the poleward direction. The time-and-zonal mean tropopause in the extratropics could probably be represented by a line joining the major axes of the ellipses of K maxima.

It might be seen from Figure 3b that the maximum of K in October 1969 occurred at 50N. This maximum is entirely due to the PFJ since "the Subtropical Jet Stream essentially outlines the poleward limit of the tropical cell of the general circulation" (Riehl, 1962, p. 30) and this limit never seems to be northward of 40 N (see Krishnamurti, 1961; and   Oort and Rasmusson, 1971, p. 23 to 24). Thus the time-and-zonal mean location of the PFJ in October 1969 was approximately 50N, whereas it was (again, approximately) 40N in January 1970. Such a large change is not likely to be anomalous. Hence we add the following remark to those made above, although this has to be verified by several more years of data analysis:

7) The PFJ tends to migrate toward the latitude of the STJ when the latter appears in the extratropical troposphere as the mean meridional circulation of the tropics intensifies in winter.

The distribution of K in APRIL (Figure 3d) has considerable semblance to the distribution of K in January. But the midlatitude maximum of K in the jet stream layer has broadened and extends to almost 65N and the bifurcation of midlatitude and subpolar maxima of K occurs (approximately) over the latitude belt 65N to 70N. The subpolar

maximum again occurs at lower altitudes than the midlatitude maximum but the structure of this maximum is not completely known since our data do not extend beyond 75N.

An important feature of the midlatitude upper tropospheric maximum of K in April 1970 is that the maximum value observed is at 300 mb at 45N and has a magnitude of $4.96 \times 10^{-5} s^{-1}$ as read from our computer output. At the 250 mb level (for which a special analysis was performed for this month) the observed maximum is again at 45N but has a magnitude of $4.8 \times 10^{-5} s^{-1}$. Thus the April maximum of K is entirely due to the PFJ which normally occurs at about the 300 mb level. However, the remnants of the STJ still linger in the atmosphere as might be seen from the distribution of the $4.5 \times 10^{-5} s^{-1}$ isopleth in the latitude belt 35N to 55N, as well as the general upward slope of the K isopleths in the equatorward direction just as in January. The separation of the K maxima associated with the STJ and the PFJ is quite conspicuous in Fig. 3d. Hence we make the following inference:

8) As the Hadley cell begins to weaken in spring the STJ also weakens; and the PFJ migrates poleward and away from the region of occurrence of the STJ. Simultaneously, the AFJ also moves poleward.

From the above, the following statements could be made concerning the time-and-zonal average location of the PFJ:

9) The southernmost location of the PFJ is in winter, and is approximately 40N. In the transitional seasons as well as in summer it occurs at approximately 45N to 50N. In these seasons the relatively broad distribution of the K maxima indicates the significant meanders of the PFJ.

The above observation is completely verified by the geographical distributions of $\{\zeta_g\}_{(t)}$ and $[\zeta_g]_{(t)}$ (see section 8) at the jet-stream

level, from which it is seen that the extratropical land masses are dominated in the transitional seasons by maxima of $\{\zeta_g\}_{(t)}$ which are essentially due to transient eddies. Thus:

10) The observation of synoptic meteorologists that the extratropical cyclones of the transitional seasons are much more intense than those of winter is seen to be valid.

7C. <u>A historical perspective: Some early results of Rossby</u>

The splitting of the Extratropical Frontal Jet Stream and the separate occurrence of Arctic Fronts and Polar Fronts have been known to synoptic meteorologists for a long time. But the interest in the study of the long term zonal circulation $[u]_{(t,\lambda)}$ has attracted meteorologists to study parameters such as $[u]_{(t,\lambda)}$, $[v]_{(t,\lambda)}$, $[w]_{(t,\lambda)}$ etc. The distribution of $[u]_{(t,\lambda)}$ has a single maximum in every calendar month which occurs in the upper troposphere. Peculiarly enough, even the parameter $[\frac{1}{2}(u^2 + v^2)]_{(t,\lambda)}$ which considers the moduli of the horizontal components of the wind tends to have a single maximum in the northern hemisphere troposphere (see Oort and Rasmusson, 1971, p.88-89). These results have led to the assumption that there is only a single zone of concentration of baroclinicity in the atmosphere. The frontal jet streams were assumed to have such large meanders that they would not appear in mean distributions such as that of $[u]_{(t,\lambda)}$.

This is indeed the case. But the distribution of the parameter K clearly brings out the presence of two jet-stream related maxima of monthly normal vorticity in the upper troposphere in winter and spring.

Rossby (1949) was able to obtain these two jet streams in a time-mean (but not zonal-mean) cross-section. He considered the geostrophic

zonal wind distribution in a vertical-meridional cross-section over
North America analyzed by Dr. S. L. Hess. This diagram is reproduced
here as Fig. 3f. Rossby plotted the data from this diagram at the 12 Km
level as a latitude vs. Rossby number diagram, which is reproduced
here as Figure 3g. This diagram indicates the presence of two jet stream-
related $[u_g]_{(t)}$ maxima in the extratropics. It might be noted that these
two maxima coincide with the K maxima at the 200 mb level in January 1970,
presented here as Figure 3h.

Rossby (op. cit.) commented as follows on these maxima: "It is of
interest to note that the averaging process has not fully erased the
sharpness of the jet. There is also some evidence for a second, weaker
jet located in about latitude 55^ON. To some extent this second jet may be
the statistical result of averaging over a large number of jet positions;
but inspection of available upper-level charts suggests that the simultaneous
occurrence of two jets is not uncommon."

8. The Geographical Distributions of $[\zeta_g]_{(t)}$ and $\{\zeta_g\}_{(t)}$

We shall consider these two types of distributions together. In
Figures 4a to 4d the distributions of $[\zeta_g]_{(t)}$ for the four months considered.
are presented and in Figures 5a to 5d those of $\{\zeta_g\}_{(t)}$. All these distri-
butions are for the 300 mb level, or approximately the level of the
Polar Front Jet Stream. As discussed in section 6 above (see also Paper A)
the distributions of $[\zeta_g]_{(t)}$ do not include transient eddies whereas those
of $\{\zeta_g\}_{(t)}$ do include them. Thus the difference

$$\{\zeta_g\}_{(t)} - |[\zeta_g]_{(t)}|$$

is a measure of the time-mean magnitude of the transient eddy vorticity
at any given location (ϕ, λ, p).

Hence a simultaneous consideration of the $[\zeta_g]_{(t)}$ and $\{\zeta_g\}_{(t)}$ fields
should enhance our knowledge of the relative importance of transient
eddies in different regions of the extratropics of the Northern Hemisphere
at the level of the PFJ.

JULY (Figures 4a and 5a)

We shall first consider the latitudinal belt 25N to 40N. In this
belt the isopleth that occurs most commonly in the $[\zeta_g]_{(t)}$ field is the
$2 \times 10^{-5} s^{-1}$ one, with the exception of West Asia and the Mediterranean Sea
region.

The values of $\{\zeta_g\}_{(t)}$ in the same region lie between $2.5 \times 10^{-5} s^{-1}$
and $3.5 \times 10^{-5} s^{-1}$. Thus the difference

$$\{\zeta_g\}_{(t)} - \left| [\zeta_g]_{(t)} \right|$$

is small. This is expected in view of the poleward migration of the
subtropical high pressure systems in summer, especially over the oceans
(see also Figures 2a to 2d), and the resulting reduction in the frequency
of occurrence of extratropical cyclones in the latitude belt considered.

In the same latitude belt over West Asia and the Mediterranean the
$[\zeta_g]_{(t)}$ isopleth values increase to $4 \times 10^{-5} s^{-1}$ while the isopleths of
$\{\zeta_g\}_{(t)}$ have maximum values of $5.5 \times 10^{-5} s^{-1}$ over West Asia and $6.5 \times 10^{-5} s^{-1}$
over parts of Italy, Greece and Turkey. Thus the vorticity contribution
by transient eddies is seen to be relatively small in these regions also.

In contrast to these is the region stretching from the Greenwich
Meridian to 90W and meridionally extending from 45N to about 65N. Here
the values of $[\zeta_g]_{(t)}$ are cyclonic and of an average value of about

$2.5 \times 10^{-5}s^{-1}$ whereas the $\{\zeta_g\}_{(t)}$ values have an approximate mean magnitude of $5 \times 10^{-5}s^{-1}$. Thus the transient eddy vorticity is of the same magnitude as the sum of the standing eddy and $[u_g]_{(t,\lambda)}$ field vorticity components. This is also true of northern USSR, particularly the 60N to 75N belt between 70E and 100E.

OCTOBER (Figures 4b and 5b)

The changes in the field of $\{\zeta_g\}_{(t)}$ from July to October are quite striking. The vorticity field intensifies very significantly during this period, especially over the middle latitudes. Whereas the July midlatitude maximum of $\{\zeta_g\}_{(t)}$ is over the north Atlantic, the October maxima seem to be very pronounced over land. Thus the maximum at 110W, 40N (over Utah in the USA) has a value in excess of $8 \times 10^{-5}s^{-1}$; over a large portion of the Hudson Bay the values of $\{\zeta_g\}_{(t)}$ exceed $6 \times 10^{-5}s^{-1}$; just east of the Urals a maximum of nearly $8 \times 10^{-5}s^{-1}$ is seen; and just west of the Sea of Japan, over the People's Republic of China, there is another maximum of value $7 \times 10^{-5}s^{-1}$. In contrast to these the only pronounced maximum over the Oceans (the Aleutian Low) is located over the northern Pacific and reaches a maximum value of nearly $8 \times 10^{-5}s^{-1}$. The values of $[\zeta_g]_{(t)}$ in these regions are observed to be rather small, ranging from $2 \times 10^{-5}s^{-1}$ to $4 \times 10^{-5}s^{-1}$, the sole exception being the North Pacific region where $[\zeta_g]_{(t)}$ values reach a maximum of nearly $6 \times 10^{-5}s^{-1}$. Thus almost all of the important maxima of $\{\zeta_g\}_{(t)}$ over land are due to transient eddies whereas the maximum over the Pacific owes itself to the vorticity of the standing eddies since that of $[u_g]_{(t,\lambda)}$ is quite small (see Figure 1b). This is probably due to the steadiness of the PFJ in this region.

Figures 6 and 7 might be considered in this connection. They are

distributions of geopotential height at the 300 mb level on 17 October

1969 and 30 October 1969 respectively. These patterns are rather typical

of the daily 300 mb height fields in this month. The height fields on

the two days presented here are seen to be typical of low index type

circulation and the jet stream systems are northward of 30 N. These

Figures had been discussed further above (see section 7).

Another important feature of Figure 4b is the cyclonic vorticity

observed over northern India. In July the observed time-mean vorticity

is anticyclonic (see Figure 4a), and provides ventilation for the air

converging into the monsoonal trough below. With the retreat of the

southwest monsoon upper-level cyclonic conditions are seen to be re-

established. The remnants of the summer anticyclone over Tibet are, however,

still observed in October. From Figures 4b and 5b it is seen that one

half or more of the temporal r.m.s. vorticity over northern India is due

to transient eddies.

APRIL (Figures 4d and 5d)

This spring month has characteristics which could be identified with

one or the other of the three other months considered.

The remnants of the 3 wave pattern of January are still discernible:

In the field of $[\zeta_g]_{(t)}$ the maximum over southern Asia and the Mediterranean

has disappeared. However, the lows over the east coasts of Asia and North

America are still present -- with significant magnitudes: Over both the

Atlantic and the Pacific the maxima exceed $5 \times 10^{-5} s^{-1}$ -- but are displaced

into the oceanic regions.

Over northern India the intense cyclonic vorticity ($[\zeta_g]_{(t)} > 3 \times 10^{-5} s^{-1}$)

of January has been replaced by near-neutral ($[\zeta_g]_{(t)} \approx 0.7 \times 10^{-5} s^{-1}$ at 80E, 35N)

conditions, and the very beginnings of the summer anticyclone over Tibet are

visible (the area covered is very small and the intensity slightly

in excess of-2 x $10^{-5}s^{-1}$). Other features of the July distribution of

$[\zeta_g]_{(t)}$ are also present: For example, the subtropical high pressure

system has moved quite northward over the Pacific, off the North

American coast.

Despite all these, April seems to resemble October most, especially

in the continental distribution of $[\zeta_g]_{(t)}$ and $\{\zeta_g\}_{(t)}$. Extremely

large values of $\{\zeta_g\}_{(t)}$ are observed over land: Over California the

$\{\zeta_g\}_{(t)}$ maximum has a value in excess of 7 x $10^{-5}s^{-1}$; in the vicinity of

the Great Lakes the highest isopleth observed is 6 x $10^{-5}s^{-1}$; over

Greenland the maximum exceeds 7 x $10^{-5}s^{-1}$; over the Mediterranean Sea

and Europe the maxima exceed 5 x $10^{-5}s^{-1}$; and near Japan there is a

maximum of value 5 x $10^{-5}s^{-1}$. One feature that distinguishes these

maxima is the observed values of $[\zeta_g]_{(t)}$ in these regions, which range

from zero to 2 x $10^{-5}s^{-1}$. Thus all of the $\{\zeta_g\}_{(t)}$ maxima over land

are due to transient eddies. This might be contrasted against the

constitution of the oceanic maxima mentioned above. The maximum

value of $\{\zeta_g\}_{(t)}$ for the Atlantic "low" (off Newfoundland) is 6.8 x $10^{-5}s^{-1}$

and the maximum value of $[\zeta_g]_{(t)}$ in the same location is 5.3 x $10^{-5}s^{-1}$;

similarly the highest value of $\{\zeta_g\}_{(t)}$ south of Kamchatka is nearly

8 x $10^{-5}s^{-1}$ and the maximum value of $[\zeta_g]_{(t)}$ here is 5.5 x $10^{-5}s^{-1}$. Thus

both of the oceanic maxima of $\{\zeta_g\}_{(t)}$ seem to owe their existence to

standing eddies (the contribution by the distribution of $[\zeta_g]_{(t,\lambda)}$ being

very small as seen from Figure 1d).

Thus the maxima of $\{\zeta_g\}_{(t)}$ over land and ocean have distinctly

different amounts of contribution by standing eddies and transient

eddies, the differences between the two types being the same in

October and April.

JANUARY (Figures 4c and 5c)

These have already been discussed in Paper A. Here we shall merely summarize the conclusions made there, and relate them to the observed features of the $[\zeta_g]_{(t)}$ and $\{\zeta_g\}_{(t)}$ distributions of the other 3 months studied.

One outstanding feature of the January distribution of $[\zeta_g]_{(t)}$ is the very intense 3 wave pattern that dominates the middle latitudes. The cyclonic vorticity maxima imbedded in this 3 wave pattern have a quasi-zonal distribution and are very sharply cutoff inland. The absolute maxima of $[\zeta_g]_{(t)}$ and especially of $\{\zeta_g\}_{(t)}$ tend to occur exactly over the coasts of Asia and North America, in the case of the oceanic extrema. The maximum $[\zeta_g]_{(t)}$ over southern Asia has a single extremal isopleth of value 5 x 10^{-5} s^{-1} over India; but when the transient eddy contributions of vorticity are added to this distribution two extremal isopleths each of value 5 x $10^{-5}s^{-1}$ appear over India and the Mediterranean, as seen from the $\{\zeta_g\}_{(t)}$ distribution of Figure 5c.

A comparison of Figures 4c and 5c shows that both the oceanic maxima of $\{\zeta_g\}_{(t)}$ are composed largely of stationary eddies and the vorticity of the long term zonal circulation. The latter is of significance only in January and then only in the midlatitudes (see Fig. 1c). The maximum of $\{\zeta_g\}_{(t)}$ over India is also composed essentially of these constituents. But the maxima of $\{\zeta_g\}_{(t)}$ over the Mediterranean, Scandinavia and northern USSR are all composed largely of transient eddies. If all these three $\{\zeta_g\}_{(t)}$ maxima were considered to be inland maxima and the maximum over India considered as a non-typical inland maximum, then the following generalization could be made concerning the componental contribution to the $\{\zeta_g\}_{(t)}$ maxima:

Except in summer all the oceanic maxima of $\{\zeta_g\}_{(t)}$ are essentially due to the vorticity of the standing eddies and of $[\zeta_g]_{(t,\lambda)}$; and all the inland maxima are essentially due to the vorticity of the transient eddies. The reverse is true in summer. Hence the observed componental constitution of $\{\zeta_g\}_{(t)}$ maxima is not due to variations in the density of the radiosonde network system over oceans and land masses.

The above remarks lead to the conclusion that in general the normal (or temporal r.m.s.) vorticity of the jet-stream level winds over land are no smaller than that observed over the oceans. However, the continental maxima of normal vorticity are generally not observed in conventional climatological maps for the simple reasons that these are arithmetic averages which eliminate the transient eddies, and that the continental maxima of normal vorticity are composed largely of transient eddies. Surely, then, our knowledge of the earth's climate is increased by a study of the temporal r.m.s. values of parameters such as vorticity.

9. Conclusions and Recommendations

Northern hemisphere geopotential height distributions of the 700 mb; 500 mb; 400 mb; 300 mb; 200 mb; and 100 mb surfaces in four months typical of the four seasons of the year have been used in a study of the geostrophic relative vorticity (ζ_g) distribution in the lower atmosphere.

The temporal arithmetic mean of ζ_g is immediately seen to be superior to the time-mean geopotential height in depicting *some* deviations from the mean zonal flow. (For the 500 mb monthly-mean geopotential height fields in January and July and a discussion of these please see Palmen and Newton, 1969, p. 67-69.)

However, only the temporal r.m.s. fields of ζ_g are capable of portraying *all* of the deviations from the zonal-mean flow. This is due to the reasons that the time-mean fields do not include transient eddies,

and that the *continental maxima* of monthly-normal (or r.m.s.) vorticity are constituted largely of transient eddies in the transitional seasons and winter. (In July *oceanic maxima* are thus constituted.)

Thus a full understanding of the eddy distributions in the atmosphere would not be obtained with the help of time-mean charts alone.

It is recommended that future climatological atlases include the temporal r.m.s. fields of parameters -- such as vorticity -- which are capable of describing the temporal normal eddy fields in the different seasons.

The zonal average of the temporal r.m.s. values of ζ_g -- the parameter K -- is shown to be a parameter which could be used to locate the zones in which the different extratropical jet streams are most commonly (or least commonly, as the case may be) observed.

The distributions of K in the four months studied indicate: 1) that there are at least three jet streams in the extratropical troposphere in January and April, 2) that there is probably only one jet stream in the extratropical troposphere in July and October, 3) that the PFJ moves toward the latitude of occurrence of the STJ when the latter appears in the winter atmosphere in conjunction with the intensification of the Hadley Cell, 4) that the PFJ moves poleward and away from the STJ when the latter weakens in spring and 5) that, as a consequence, the highest values of K in the upper troposphere over the latitude belt 45N to 55N are observed in the months of April and October.

ACKNOWLEDGEMENTS

REFERENCES

Gray, William M., 1972. Cumulus Convection and Larger-scale Circulations, Part III: Broadscale and Mesoscale Considerations. Atmospheric Science Paper No. 190, Dept. of Atmospheric Science, Colorado State University, Fort Collins, Colorado, 80pp.

Krishnamurti, Tiruvalem N., 1961. The Subtropical Jet Stream of Winter, J. Meteorol., 18:172-191.

Lorenz, Edward N., 1967. The Nature and Theory of the General Circulation of the Atmosphere, World Meteorological Organization, No. 218. TP. 115, 161pp.

Mahlman, J. D., 1967. Further Studies on Atmospheric General Circulation and Transport of Radioactive Debris, Atmospheric Science Paper No. 110, Dept. of Atmospheric Science, Colorado State University, Fort Collins, Colorado, 68 pp.

Oort, Abraham H., and Eugene M. Rasmusson, 1971. Atmospheric Circulation Statistics, NOAA Professional Paper 5, (U. S. Govt. Printing Office, Washington, D. C. Stock Number 0317-0045). 323 pp.

Palmen, E., and C. W. Newton, 1969. Atmospheric Circulation Systems: Their Structure and Physical Interpretation, Academic Press, New York and London, 603 pp.

Reiter, Elmar R., 1969a. Mean and Eddy Motions in the Atmohphere. Mon. Wea. Rev., 97:200-204.

Reiter, Elmar R., 1969b. Atmospheric Transport Processes, Part 1: Energy Transfers and Transformations. TID-24868, U. S. Atomic Energy Commission, Division of technical Information Extension, Oak Ridge, Tenn. 253 pp.

Reiter, Elmar R., 1972. Atmospheric Transport Processes, Part 3: Hydrodynamic Tracers. TID-25731, U. S. Atomic Energy Commission, Division of Technical Information Extension, Oak Ridge, Tenn. 212 pp.

Reiter, Elmar R., M. E. Glasser, and J. D. Mahlman, 1967. The Role of the Tropopause in Stratospheric-Tropospheric Exchange Processes. Atmospheric Science Paper No. 107, Dept. of Atmospheric Science, Colorado State University, Fort Collins, Colo., 60 pp.

Reiter, Elmar R., and L. F. Whitney, 1969. Interaction Between Subtropical and Polar-Front Jet Stream. Mon. Wea. Rev., 97:432-438.

Riehl, Herbert, 1962. Jet Streams of the Atmosphere, Technical Report No. 32, Dept. of Atmospheric Science, Colorado State University, Fort Collins, Colo., 117 pp.

Rossby, Carl-Gustaf, 1949. On the Nature of the General Circulation
of the Lower Atmosphere, Chapter II, p. 16-48 *in the* Atmospheres
of the Earth and Planets (Kuiper, Ed.) The University of Chicago
Press, 366 pp.

Srivatsangam, Srinivasan, 1973. A Contribution to the Synoptic
Climatology of the Extratropics. Atmospheric Science Paper No. 203,
Dept. of Atmospheric Science, Colorado State University,
Fort Collins, Colo., 34 pp.

U. S. Dept. of Commerce, 1962-63. Daily Aerological Cross Sections:
Pole to Pole along Meridian 75°W for the IGY Period (July 1957 to
Dec. 1958). For sale by the Superintendent of Documents, U. S.
Govt. Printing Office, Washington, D. C. Price (each month) $1.75.

APPENDIX 1a

$[\{\zeta_g\}_{(\lambda)}]_{(t)}$ and $[\{\zeta_g\}_{(t)}]_{(\lambda)}$ for July 1969

Units: $10^{-7}s^{-1}$

(For an explanation of symbols see Table 1)

$[\{\zeta_g\}_{(\lambda)}]_{(t)}$

PRES mb	25N	30N	35N	40N	45N	50N	55N	60N	65N	70N	75N
700	148	143	155	145	165	195	195	201	189	172	184
500	177	174	211	213	236	270	267	270	255	248	249
400	199	217	257	274	300	354	324	330	310	307.	302
300	239	283	333	372	401	425	402	405	377	373	358
200	297	343	387	438	430	423	349	313	262	242	227
100-	234	217	207	165	152	139	121	103	88	74	78

$[\{\zeta_g\}_{(t)}]_{(\lambda)}$

PRES mb	25N	30N	35N	40N	45N	50N	55N	60N	65N	70N	75N
700	144	·140	151	146	167	191	188	200	190	175	192
500	174	173	206	213	238	266	261	271	258	251	261
400	195	214	253	273	302	326	318	332	313	311	314
300	235	280	326	371	401	415	395	411	382	376	372
200	291	340	379	439	431	421	345	319	263	248	238
100	212	210	195	167	151	140	117	103	90	81	81

APPENDIX 1b

Same as Appendix 1a But for October 1969

$[\{\zeta_g\}_{(\lambda)}]_{(t)}$

PRES mb	25N	30N	35N	40N	45N	50N	55N	60N	65N	70N	75N
700	162	175	179	193	229	259	·243	227	195	179	189
500	204	237	263	289	349	372	343	319	274	255	257
400	238	288	318	361	437	463	428	391	341	313	308
300	277	357	386	433	522	558	502	457	402	373	360
200	313	387	418	442	492	482	402	356	309	277	261
100	228	215	212	189	202	193	177	166	159	149	142

$[\{\zeta_g\}_{(t)}]_{(\lambda)}$

PRES mb	25N	30N	35N	40N	45N	50N	55N	60N	65N	70N	75N
700	157	167	177	186	219	251	235	220	192	178	186
500	199	227	259	280	338	364	335	315	277	254	261
400	235	278	309	351	420	454	419	386	346	315	313
300	275	347	375	423	504	549	494	453	408	375	364
200	311	377	408	432	474	474	395	351	312	279	264
100	223	209	208	185	195	191	173	163	159	152	146

APPENDIX 1c

Same as Appendix 1a But for April 1970

$$[\{\zeta_g\}_{(\lambda)}]_{(t)}$$

PRES mb	25N	30N	35N	40N	45N	50N	55N	60N	65N	70N	75N
700	157	176	185	194	240	253	226	198	182	169	206
500	218	247	284	284	351	344	306	286	267	262	320
400	270	310	353	363	434	419	376	350	326	322	376
300	332	385	430	444	510	488	426	393	352	343	364
200	368	423	453	439	441	388	301	266	224	222	229
100	236	214	206	202	182	170	143	118	112	123	136

$$[\{\zeta_g\}_{(t)}]_{(\lambda)}$$

PRES mb	25N	30N	35N	40N	45N	50N	55N	60N	65N	70N	75N
700	152	172	183	190	229	246	223	196	177	164	205
500	213	244	281	281	338	338	302	281	260	258	312
400	266	306	349	358	421	413	372	344	319	317	367
300	327	381	427	440	496	483	425	388	346	337	355
200	363	420	451	435	427	380	298	262	219	215	222
100	233	209	204	198	174	164	140	115	108	116	132

)

APPENDIX 2

$[H]_{(t,\lambda)}$ for the 4 Months analyzed. Units: Geopotential Meters.

JULY 1969

LAT	700 MB	500 MB	300 MB	200 MB	100 MB
0 N	3147.7	5852.7	9665.0	12396.0	16562.0
5 N	3176.0	5885.5	9694.5	12438.5	16608.5
10 N	3155.0	5878.0	9706.7	12455.3	16643.6
15 N	3145.7	5864.6	9691.7	12421.7	16633.1
20 N	3160.5	5892.7	9703.8	12436.1	16629.7
25 N	3170.8	5899.2	9710.9	12450.5	16666.0
30 N	3176.2	5898.9	9710.7	12453.6	16691.4
35 N	3172.1	5885.1	9681.7	12420.8	16691.9
40 N	3153.2	5843.1	9604.9	12330.9	16659.5
45 N	3119.6	5782.6	9503.3	12204.9	16606.5
50 N	3079.7	57.8.6	9401.0	12081.1	16551.9
55 N	3042.7	5661.6	9315.3	11987.2	16507.7
60 N	3011.0	5612.0	9239.2	11910.3	16478.3
65 N	2994.4	5582.3	9190.6	11863.7	16461.4
70 N	2978.2	5557.4	9156.7	11831.2	16449.5
75 N	2951.4	5518.6	9105.1	11791.6	16436.4
80 N	2916.0	5463.8	9031.7	11739.8	16419.3
AVG HGT	3091.2	5752.7	9477.2	12189.0	16570.4

OCTOBER 1969

LAT	700 MB	500 MB	300 MB	200 MB	100 MB
0 N	3137.3	5845.7	9662.0	12400.3	16510.0
5 N	3161.0	5880.0	9704.0	12452.0	16639.0
10 N	3149.4	5864.4	9688.3	-12430.6	16625.6
15 N	3153.5	5868.6	9688.5	12428.3	16598.6
20 N	3153.4	5870.3	9663.7	12377.5	16547.1
25 N	3152.6	5857.5	9632.6	12338.7	16530.2
30 N	3142.1	5827.1	9570.5	12264.3	16492.4
35 N	3119.7	5777.5	9481.3	12153.9	16427.8
40 N	3083.4	5704.6	9364.2	12017.0	16339.3
45 N	3029.9	5610.8	9223.1	11862.4	16237.3
50 N	2971.9	5520.8	9085.5	11716.3	16138.9
55 N	2923.4	5446.6	8973.3	11596.9	16050.9
60 N	2884.1	5385.6	8882.9	11498.5	15970.6
65 N	2856.8	5342.8	8820.0	11425.7	15898.2
70 N	2829.4	5297.7	8755.3	11355.1	15831.8
75 N	2801.7	5250.4	8684.9	11286.2	15771.7
80 N	2784.9	5218.8	8635.2	11237.8	15724.7
AVG HGT	3019.7	5621.7	9265.6	11931.9	16254.9

APRIL 1970

LAT	700 MB	500 MB	300 MB	200 MB	100 MB
0 N	3144.7	5862.7	9693.7	12452.7	16589.0
5 N	3170.0	5900.0	9751.3	12469.0	16766.3
10 N	3159.0	5887.7	9728.5	12491.2	16694.5
15 N	3163.2	5879.8	9694.5	12436.5	16632.0
20 N	3163.7	5875.7	9654.4	12356.4	16566.0
25 N	3155.4	5847.4	9595.5	12281.8	16495.1
30 N	3131.4	5793.3	9497.6	12164.3	16419.7
35 N	3100.2	5723.6	9376.3	12015.4	16323.9
40 N	3056.2	5640.4	9239.5	11859.2	16223.6
45 N	2998.2	5545.3	9098.8	11711.9	16126.4
50 N	2945.8	5463.2	8979.3	11588.7	16041.2
55 N	2904.8	5398.0	8882.9	11491.2	15970.3
60 N	2868.3	5338.3	8794.8	11408.9	15912.2
65 N	2837.4	5285.6	8717.9	11338.4	15861.9
70 N	2809.9	5227.2	8632.9	11266.7	15814.3
75 N	2791.3	5178.1	8559.6	11205.1	15772.6
80 N	2784.6	5158.1	8521.9	11168.0	15743.5
AVG HGT	3010.8	5588.5	9201.1	11865.0	16232.5

JANUARY 1970

LAT	700 MB	500 MB	300 MB	200 MB	100 MB
0 N	3145.7	5857.7	9674.7	12407.7	16536.0
5 N	3166.7	5886.3	9710.7	12456.3	16662.3
10 N	3156.3	5872.4	9692.1	12426.7	16625.4
15 N	3156.5	5866.4	9669.0	12391.2	16578.0
20 N	3152.5	5843.0	9603.4	12303.0	16497.6
25 N	3125.4	5783.9	9503.8	12188.2	16414.9
30 N	3077.1	5693.0	9347.5	12004.5	16284.9
35 N	3015.5	5582.7	9163.1	11778.4	16126.5
40 N	2949.2	5469.4	8984.6	11576.7	15972.6
45 N	2891.3	5377.3	8847.6	11427.8	15840.8
50 N	2852.4	5315.9	8757.4	11324.1	15734.4
55 N	2825.5	5270.0	8688.3	11249.1	15656.2
60 N	2802.9	5227.6	8629.0	11193.2	15601.9
65 N	2796.9	5204.4	8594.3	11161.7	15571.4
70 N	2797.6	5193.8	8571.8	11141.3	15561.2
75 N	2794.6	5182.5	8552.5	11127.3	15565.8
80 N	2781.6	5157.7	8526.5	11112.6	15576.2
AVG HGT	2969.9	5516.7	9089.2	11721.8	16047.4

APPENDIX 3

$$[u_g]_{(t,\lambda)} \text{ Calculated from } [!!]_{(t,\lambda)} \text{ in Appendix 2}$$

Units: ms^{-1}

JULY 1969

DEG. LAT. NORTH

PRES mb	17.5	22.5	27.5	32.5	37.5	42.5	47.5	52.5	57.5	62.5	67.5	72.5	77.5
700	-6.0	-3.3	-1.4	.9	3.8	6.0	6.5	5.6	4.5	2.3	2.1	3.4	4.4
500	-11.3	-2.1	.1	3.1	8.3	10.8	10.5	8.7	7.1	4.1	3.3	4.9	6.8
300	-4.9	-2.2	.1	6.5	15.3	18.2	16.8	13.1	10.9	6.6	4.4	6.5	9.1
.200	-5.8	-4.6	-.8	7.4	17.9	22.6	20.3	14.3	11.0	6.4	4.3	5.0	6.4
100	1.4	-11.5	-6.7	-.1	6.4	9.5	9.0	6.7	4.2	2.3	1.6	1.7	2.1

OCTOBER 1969

DEG. LAT. NORTH

PRES mb	17.5N	22.5N	27.5N	32.5N	37.5N	42.5N	47.5N	52.5N	57.5N	62.5N	67.5N	72.5N	77.5N
700	.0	.3	2.8	5.0	7.2	9.6	9.5	7.4	5.6	3.7	3.6	3.5	2.1
500	-.7	4.0	8.0	11.2	14.5	16.8	14.8	11.3	8.7	5.8	5.9	6.0	3.9
300	10.0	9.8	16.3	20.1	23.3	25.3	22.6	17.1	13.0	8.6	8.5	8.9	6.2
200	20.4	12.3	19.5	24.9	27.2	27.7	24.0	18.2	14.1	9.9	9.2	8.7	6.0
100	20.7	5.3	9.9	14.5	17.6	18.3	16.1	13.4	11.5	9.9	8.7	7.6	5.8

JANUARY 1970

DEG. LAT. NORTH

PRES mb	17.5N	22.5N	27.5N	32.5N	37.5N	42.5N	47.5N	52.5N	57.5N	62.5N	67.5N	72.5N	77.5N
700	1.6	8.6	12.7	13.9	13.2	10.4	6.4	4.1	3.2	.8	-.1	.4	1.6
500	9.4	18.7	23.8	24.8	22.5	16.5	10.1	7.0	6.1	3.2	1.4	1.4	3.1
300	26.4	31.5	40.9	41.5	35.5	24.5	14.8	10.5	8.5	4.7	2.9	2.4	3.2
200	35.5	36.3	48.1	50.9	40.1	26.7	17.0	11.4	8.0	4.3	2.7	1.8	1.8
100	32.3	26.1	34.1	35.7	30.6	23.6	17.5	11.9	7.8	4.2	1.3	-.6	-1.3

APRIL 1970

DEG. LAT. NORTH

PRES mb	17.5	22.5	27.5	32.5	37.5	42.5	47.5	52.5	57.5	62.5	67.5	72.5	77.5
700	-.2	2.6	6.3	7.0	8.7	10.4	8.6	6.3	5.2	4.2	3.6	2.4	.8
500	1.6	8.9	14.2	15.7	16.5	17.0	13.5	9.9	8.6	7.2	7.6	6.2	2.5
300	16.1	18.6	25.6	27.3	27.2	25.2	19.6	14.7	12.6	10.5	11.1	9.3	4.7
200	32.2	23.6	30.8	33.5	31.0	26.4	20.2	14.9	11.8	9.6	9.4	7.8	4.6
100	26.6	22.4	19.8	21.6	19.9	17.4	14.0	10.8	8.3	6.9	6.2	5.3	3.6

APPENDIX 4

$[\zeta_g]_{(t,\lambda)}$ Calculated from the $[u_g]_{(t,\lambda)}$ values of Appendix 3.

Units: $10^{-7}s^{-1}$

JULY 1969

PRES mb	20N	25N	30N	35N	40N	45N	50N	55N	60N	65N	70N	75N
700	-51.2	-34.9	-42.3	-48.4	-34.3	.3	27.7	31.1	50.4	9.9	-11.1	5.0
500	-170.3	-39.1	-53.1	-88.0	-32.1	22.7	50.5	46.1	70.3	26.5	-12.3	.7
300	-49.3	-42.2	-113.6	-145.2	-30.7	52.8	94.8	65.6	101.0	58.0	-14.2	-.1
200	-25.3	-69.3	-144.6	-174.8	-57.9	74.1	140.3	87.6	107.8	55.7	6.2	8.4
100	228.3	-93.4	-120.8	-114.5	-44.4	24.0	54.6	57.7	43.3	19.9	5.1	2.8

OCTOBER 1969

PRES mb	20N	25N	30N	35N	40N	45N	50N	55N	60N	65N	70N	75N
700	-3.7	-43.9	-37.7	-32.3	-31.5	16.1	54.0	46.3	47.2	14.7	16.6	42.2
500	-84.2	-66.1	-49.0	-45.7	-21.0	61.3	86.6	68.7	72.3	18.5	24.0	66.6
300	8.3	-106.3	-52.2	-53.5	-4.0	85.9	135.6	108.3	108.3	30.6	29.3	94.1
200	156.4	-118.5	-76.5	-13.7	27.5	107.3	143.2	109.9	108.0	44.6	47.9	92.5
100	284.2	-76.5	-72.5	-37.1	11.4	65.2	76.7	62.2	58.7	52.5	54.5	71.8

JANUARY 1970

PRES mb	20N	25N	30N	35N	40N	45N	50N	55N	60N	65N	70N	75N
700	-122.3	-65.8	-9.9	27.4	66.0	84.9	50.9	23.7	49.1	17.6	-7.9	-16.3
500	-158.8	-76.8	3.7	67.8	134.1	136.4	71.3	31.2	65.1	39.6	5.3	-16.3
300	-75.2	-143.9	27.1	151.2	236.5	206.1	100.4	57.9	85.9	45.1	20.6	2.7
200	6.0	-182.2	-5.1	244.9	285.5	208.0	127.0	83.3	83.7	41.0	25.7	9.7
100	128.4	-120.5	2.7	127.9	161.4	142.8	127.1	96.5	81.6	60.1	36.2	7.2

APRIL 1970

PRES mb	20N	25N	30N	35N	40N	45N	50N	55N	60N	65N	70N	75N
700	-50.2	-62.7	-7.2	-22.3	-17.0	47.1	56.1	31.2	31.2	24.2	35.2	36.9
500	-128.3	-85.6	-13.8	2.6	13.2	88.0	85.4	45.6	46.2	16.7	55.5	93.0
300	-34.8	-110.3	-5.9	32.2	70.3	135.7	120.4	67.8	70.1	24.8	77.0	124.2
200	171.5	-109.7	-20.2	80.2	121.8	147.5	129.1	85.0	68.5	36.1	65.4	94.2
100	88.5	63.3	-14.0	52.3	70.1	86.3	80.2	66.1	47.2	33.3	41.8	56.4

APPENDIX 5

$[u_g]_{(t,\lambda)}$ Calculated from the 5-year Mean Values of $[H]_{(t,\lambda)}$ Presented by Oort and Rasmusson (1971, p. 84). Units: ms^{-1}.

JULY

DEG. LAT. NORTH

PRES mb	17.5	22.5	27.5	32.5	37.5	42.5	47.5	52.5	57.5	62.6	67.5	72.5
700	1.2	-1.3	-3.1	.7	5.2	6.8	6.1	4.6	3.0	1.9	2.1	2.4
500	-2.4	-2.2	-1.3	3.6	8.9	11.1	10.2	7.3	5.2	3.7	3.7	4.1
300	-6.4	-4.1	1.3	8.8	15.5	18.1	16.1	11.6	8.2	6.3	6.2	6.6
200	-8.4	-5.7	1.6	10.1	18.3	21.8	19.0	12.8	8.7	5.7	5.1	5.7
100	-14.9	-12.0	-5.0	1.1	5.4	7.5	9.2	6.3	4.2	1.0	.8	1.8

OCTOBER

DEG. LAT. NORTH

PRES mb	17.5	22.5	27.5	32.5	37.5	42.5	47.5	52.5	57.5	62.6	67.5	72.5
700	-1.6	.3	1.8	4.5	7.0	8.8	9.5	8.7	6.7	4.8	3.7	2.7
500	-1.2	3.5	7.6	10.1	12.9	14.9	14.8	13.1	10.3	7.6	6.3	4.7
300	-.8	7.9	16.0	22.1	23.3	22.2	21.3	18.8	14.9	11.2	9.3	7.9
200	.8	8.9	19.6	27.9	28.6	25.1	22.5	19.5	15.8	11.7	10.1	8.5
100	-5.2	-.3	10.5	18.2	19.1	16.1	15.8	14.8	13.2	10.0	9.8	9.3

JANUARY

DEG. LAT. NORTH

PRES mb	17.5	22.5	27.5	32.5	37.5	42.5	47.5	52.5	57.5	62.6	67.5	72.5
700	4.4	7.9	8.6	9.9	10.9	10.0	8.2	5.9	4.3	3.0	2.4	2.0
500	10.5	17.4	19.1	19.8	19.7	16.5	12.1	8.7	6.7	5.7	4.7	4.1
300	18.5	32.6	37.5	35.8	31.4	24.4	17.6	12.5	9.2	7.8	7.2	6.3
200	22.1	37.3	45.3	44.8	36.8	26.3	19.4	14.6	11.2	9.8	9.0	7.0
100	12.1	23.7	31.2	32.6	28.6	21.7	18.0	14.5	14.8	10.9	10.7	12.3

APRIL

DEG. LAT. NORTH

PRES mb	17.5	22.5	27.5	32.5	37.5	42.5	47.5	52.5	57.5	62.6	67.5	72.5
700	2.0	4.4	5.8	7.9	8.9	8.4	6.9	5.6	4.9	4.1	3.3	2.3
500	5.2	9.8	12.6	16.2	16.7	14.1	11.2	9.1	8.2	7.2	6.0	4.7
300	14.5	21.2	25.4	26.8	25.4	21.3	16.9	14.0	12.3	10.8	9.0	6.6
200	18.9	26.9	33.3	34.2	28.8	21.8	16.9	13.7	12.0	10.0	8.2	5.8
100	11.3	15.2	20.7	23.2	19.1	13.3	10.5	9.0	8.9	7.5	6.3	4.6

APPENDIX 6

$[\zeta_g]_{(t,\lambda)}$ Calculated for the 5-year Mean Oort and Rasmusson

(1971) Data. Units: $10^{-7}s^{-1}$

JULY

DEG. LAT. NORTH

PRES mb	20	25	30	35	40	45	50	55	60	65	70
700	44.5	32.2	-69.9	-77.6	-21.6	23.3	36.9	36.6	26.5	3.4	4.0
500	-4.9	-17.5	-87.4	-89.2	-25.7	33.4	67.7	52.8	38.7	12.7	9.6
300	-44.9	-98.6	-129.9	-107.6	-24.4	62.9	106.7	83.6	53.9	23.1	19.5
200	-53.7	-132.2	-148.8	-131.1	-37.7	82.7	141.8	97.2	74.1	29.4	12.5
100	-59.4	-132.9	-111.6	-72.8	-30.3	-16.9	67.3	49.3	64.6	6.0	-12.3

OCTOBER

DEG. LAT. NORTH

PRES mb	20	25	30	35	40	45	50	55	60	65	70
700	-35.0	-26.5	-45.2	-37.8	-22.4	1.0	31.9	52.4	51.1	34.1	31.7
500	-83.7	-70.1	-37.6	-37.5	-16.7	25.0	55.8	76.4	72.8	47.8	52.3
300	-154.7	-136.7	-92.3	3.6	48.8	49.9	83.9	106.8	102.7	68.4	62.8
200	-142.1	-184.0	-127.3	18.5	99.2	83.9	92.6	106.9	110.3	66.3	68.6
100	-90.0	-190.6	-126.6	5.4	76.5	31.6	45.9	60.1	89.8	35.7	51.2

JANUARY

DEG. LAT. NORTH

PRES mb	20	25	30	35	40	45	50	55	60	65	70
700	-59.1	-7.3	-14.3	-7.0	30.0	47.1	53.9	41.1	33.4	20.6	15.4
500	-116.7	-17.9	5.3	24.2	81.4	100.4	81.6	52.4	35.2	35.8	30.7
300	-238.4	-62.7	63.2	116.2	163.5	155.2	119.1	84.1	48.4	35.5	44.7
200	-256.2	-114.2	50.2	189.6	229.5	161.2	116.8	91.1	53.2	45.9	71.6
100	-199.3	-114.3	2.5	106.2	158.2	96.3	94.6	27.6	104.5	39.6	21.5

APRIL

DEG. LAT. NORTH

PRES mb	20	25	30	35	40	45	50	55	60	65	70
700	-41.6	-20.4	-31.9	-9.9	20.9	39.5	34.2	25.6	26.5	27.1	29.8
500	-78.0	-41.8	-52.4	9.4	66.2	73.7	55.2	36.9	38.0	44.0	47.0
300	-110.4	-59.1	-1.2	53.1	105.1	109.3	80.6	60.0	59.5	64.6	77.6
200	-130.3	-95.2	13.5	132.0	158.8	119.4	85.8	59.0	67.6	61.4	73.8
100	-62.8	-86.3	-25.0	97.3	126.2	68.1	45.3	21.9	47.3	45.1	54.3

APPENDIX 7

$[\zeta]_{(t,\lambda)}$ Calculated from the $[u]_{(t,\lambda)}$ Data of Oort and
Rasmusson (1971, p. 76-77). Units: $10^{-7}s^{-1}$.

JULY

PRES mb	20N	25N	30N	35N	40N	45N	50N	55N	60N	65N	70N
700	- 15	- 21	- 34	- 31	- 17	3	28	37	22	5	1
500	- 23	- 47	- 68	- 62	- 25	23	54	54	32	11	9
300	- 25	- 59	-109	-107	- 31	56	94	82	46	20	19
200	- 42	- 71	-128	-135	- 39	70	122	109	59	26	23
100	- 52	- 94	-119	-103	- 39	23	54	52	30	11	3

OCTOBER

PRES mb	20N	25N	30N	35N	40N	45N	50N	55N	60N	65N	70N
700	- 39	- 43	- 37	- 28	- 21	- 8	21	46	49	39	29
500	- 63	- 63	- 44	- 26	- 13	8	43	67	63	49	44
300	- 92	- 86	- 52	- 9	16	39	70	88	80	63	57
200	-104	- 98	- 57	1	43	64	83	94	85	69	60
100	- 77	- 86	- 65	- 26	13	35	47	54	52	51	57

JANUARY

PRES mb	20N	25N	30N	35N	40N	45N	50N	55N	60N	65N	70N
700	- 77	- 50	- 15	15	30	39	43	37	27	21	19
500	-133	- 57	19	57	70	72	68	51	31	24	26
300	-170	- 96	30	125	146	131	101	63	39	34	39
200	-168	-109	27	150	180	149	108	69	45	40	47
100	-134	- 92	- 2	75	94	79	58	44	41	48	65

APRIL

PRES mb	20N	25N	30N	35N	40N	45N	50N	55N	60N	65N	70N
700	- 65	- 42	- 15	5	17	21	27	29	26	26	31
500	- 84	- 48	- 10	18	35	44	49	47	38	39.	50
300	-105	- 41	18	54	73	80	80	66	49	55	70
200	-123	- 53	39	108	121	102	85	69	53	54	62
100	- 94	- 61	4	59	75	65	51	38	31	35	44

APPENDIX 8

$\{\{\zeta_g\}_{(t)}\}_{(\lambda)}$ in January 1970. Units: $10^{-7}s^{-1}$.

PRES mb	25N	30N	35N	40N	45N	50N	55N	60N	65N	70N	75N
700	186	181	201	229	241	246	241	258	237	234	257
500	251	262	302	354	350	332	326	362	360	343	362
300	354	406	459	515	483	429	402	435	418	401	396
200	373	425	508	493	413	326	295	306	290	280	269
100	256	230	244	251	235	211	185	185	185	178	174

$\{\{\zeta_g\}_{(t)}\}_{(\lambda)}$ for October 1969. Units: $10^{-7}s^{-1}$.

PRES mb	25N	30N	35N	40N	45N	50N	55N	60N	65N	70N	75N
700	163	173	180	196	231	261	244	229	201	184	194
500	204	235	264	294	352	374	344	324	284	259	265
400	240	288	318	368	439	464	428	395	352	319	317
300	279	359	387	445	524	558	502	461	413	380	368
200	317	387	420	451	493	482	403	357	319	284	266
100	232	215	213	192	203	195	177	168	165	156	147

APPENDIX 9

$$\{\{\zeta_g\}_{(\lambda)}\} \ (t) \quad \text{in units:} \quad 10^{-4}s^{-1}$$

JULY 1969

PRES mb	25N	30N	35N	40N	45N	50N	55N	60N	65N	70N	75N
700	.150	.143	.157	.146	.167	.196	.197	.203	.191	.174	.189
500	.178	.175	.213	.215	.238	.274	.269	.273	.258	.250	.254
400	.200	.218	.259	.277	.303	.339	.327	.333	.313	.310	.307
300	.241	.285	.334	.375	.403	.431	.405	.408	.380	.377	.362
200	.299	.345	.388	.441	.432	.427	.350	.315	.264	.245	.230
100	.235	.222	.208	.166	.153	.140	.121	.105	.089	.076	.079

OCTOBER 1969

PRES mb	25N	30N	35N	40N	45N	50N	55N	60N	65N	70N	75N
700	.163	.177	.180	.195	.232	.262	.245	.230	.199	.183	.193
500	.205	.239	.264	.291	.353	.375	.345	.323	.281	.258	.261
400	.239	.290	.320	.364	.443	.466	.430	.395	.349	.317	.313
300	.280	.360	.388	.439	.529	.561	.505	.460	.409	.376	.364
200	.315	.390	.420	.449	.496	.486	.404	.357	.315	.281	.264
100	.229	.217	.214	.192	.204	.196	.178	.167	.164	.153	.144

JANUARY 1970

PRES mb	25N	30N	35N	40N	45N	50N	55N	60N	65N	70N	75N
700	.186	.180	.200	.226	.245	.247	.239	.252	.240	.238	.259
500	.251	.259	.300	.352	.351	.329	.321	.356	.365	.352	.369
400	.298	.334	.370	.442	.418	.388	.376	.417	.417	.398	.404
300	.355	.403	.459	.513	.486	.423	.397	.430	.425	.409	.406
200	.374	.422	.512	.492	.413	.321	.289	.304	.295	.288	.274
100	.257	.229	.245	.253	.236	.210	.182	.183	.186	.179	.173

APRIL 1970

PRES mb	25N	30N	35N	40N	45N	50N	55N	60N	65N	70N	75N
700	.158	.177	.187	.198	.243	.257	.230	.202	.184	.172	.210
500	.219	.251	.289	.292	.355	.349	.311	.291	.271	·.267	.327
400	.272	.316	.357	.370	.438	.423	.381	.354	.330	.327	.382
300	.334	.39]	.436	.453	.513	.491	.431	.396	.355	.346	.368
200	.370	.430	.457	.443	.443	.390	.304	.270	.228	.225	.231
100	.237	.216	.209	.204	.184	.171	.145	.119	.113	.124	.138

A Note on the Illustrations:

In the computer analyzed maps of $[\zeta_g]_{(t)}$ and $\{\zeta_g\}_{(t)}$ the analyses are not valid north of 75N and south of 25N, being merely extrapolations of the values at 75N and 25N respectively.
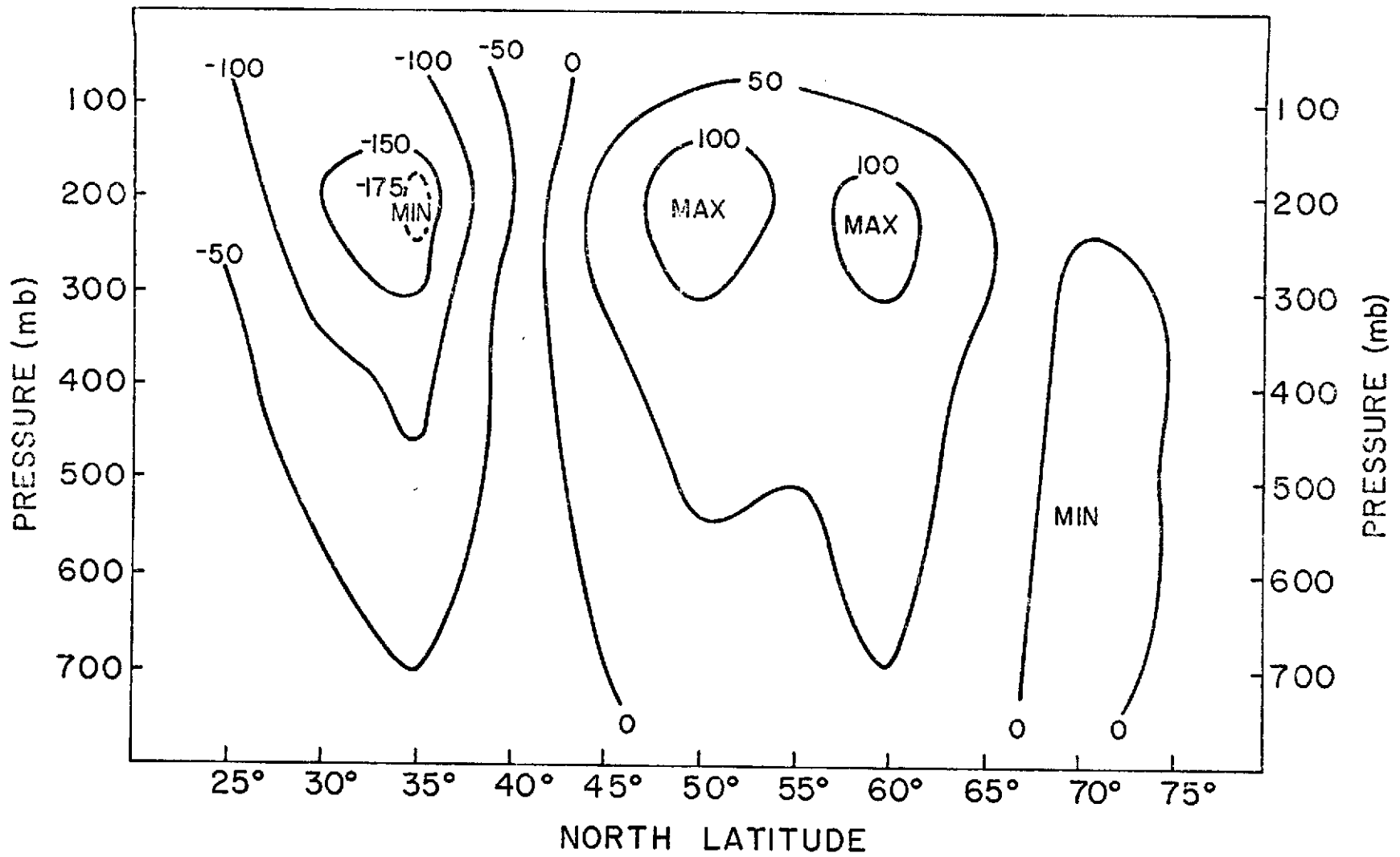
Figure 1a. The distribution of $[\zeta_g]_{(t,\lambda)}$ in July 1969. Units: $10^{-7}s^{-1}$.
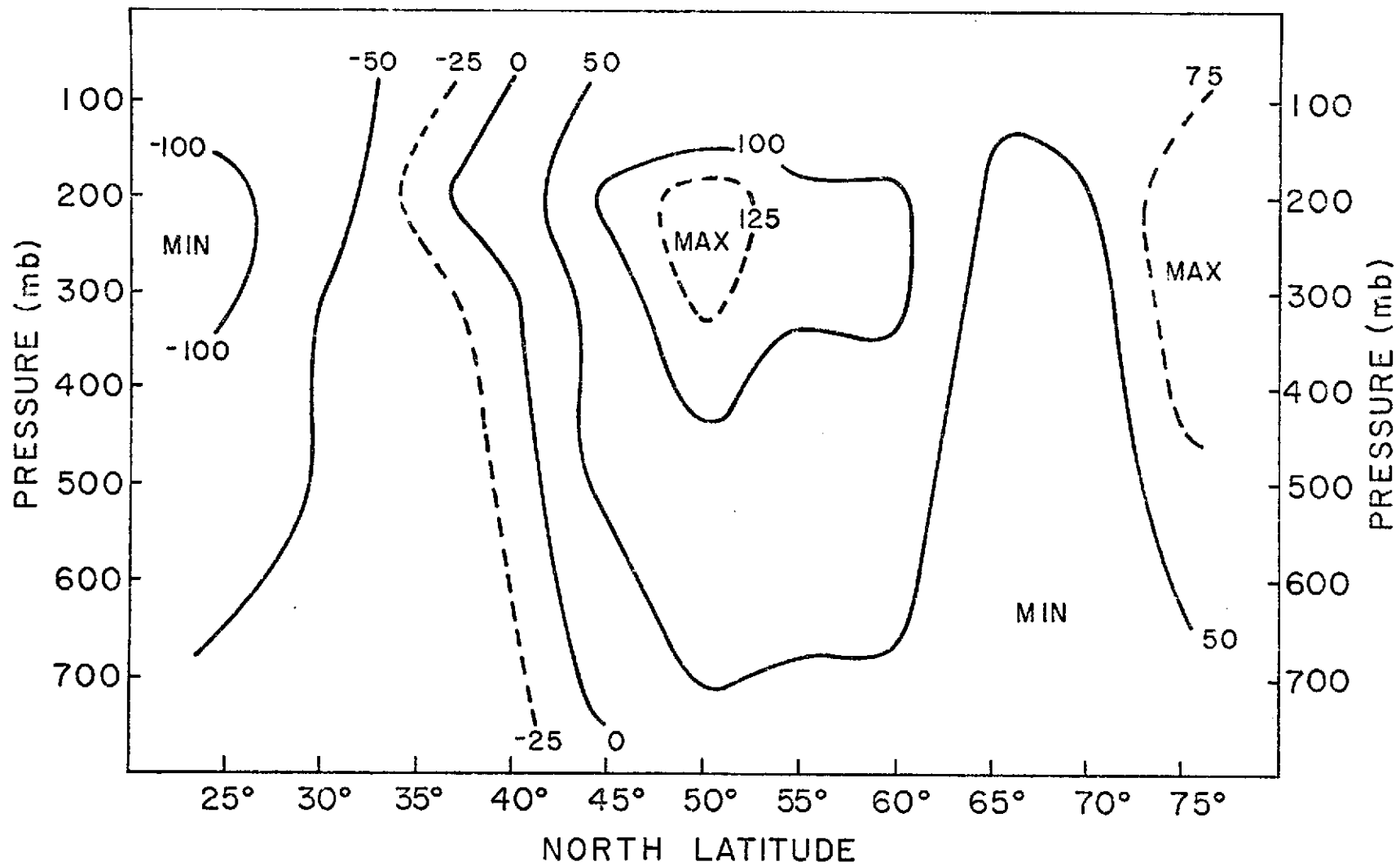
Figure 1b. The distribution of $[\zeta_g]_{(t,\lambda)}$ in October 1969. Units: $10^{-7}s^{-1}$
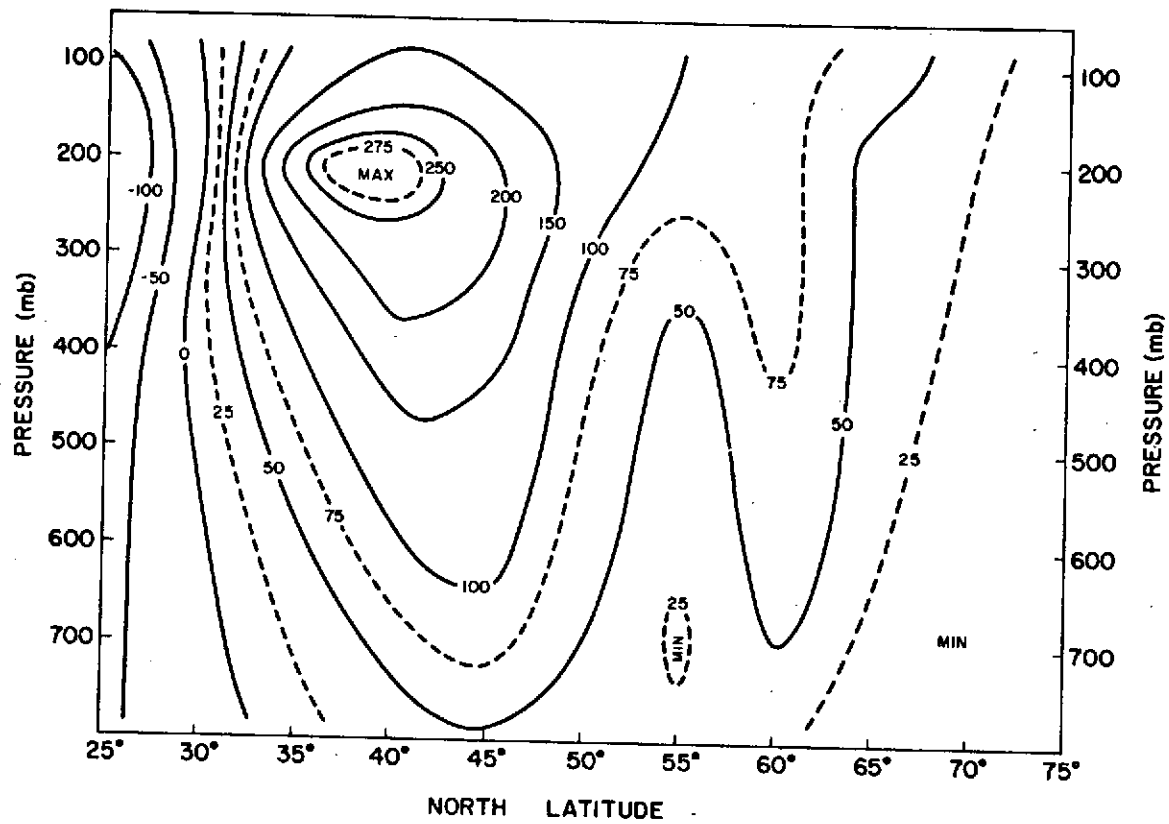
Figure 1c. The distribution of $[\zeta_g]_{(t,\lambda)}$ in January 1970. Units: $10^{-7}s^{-1}$.
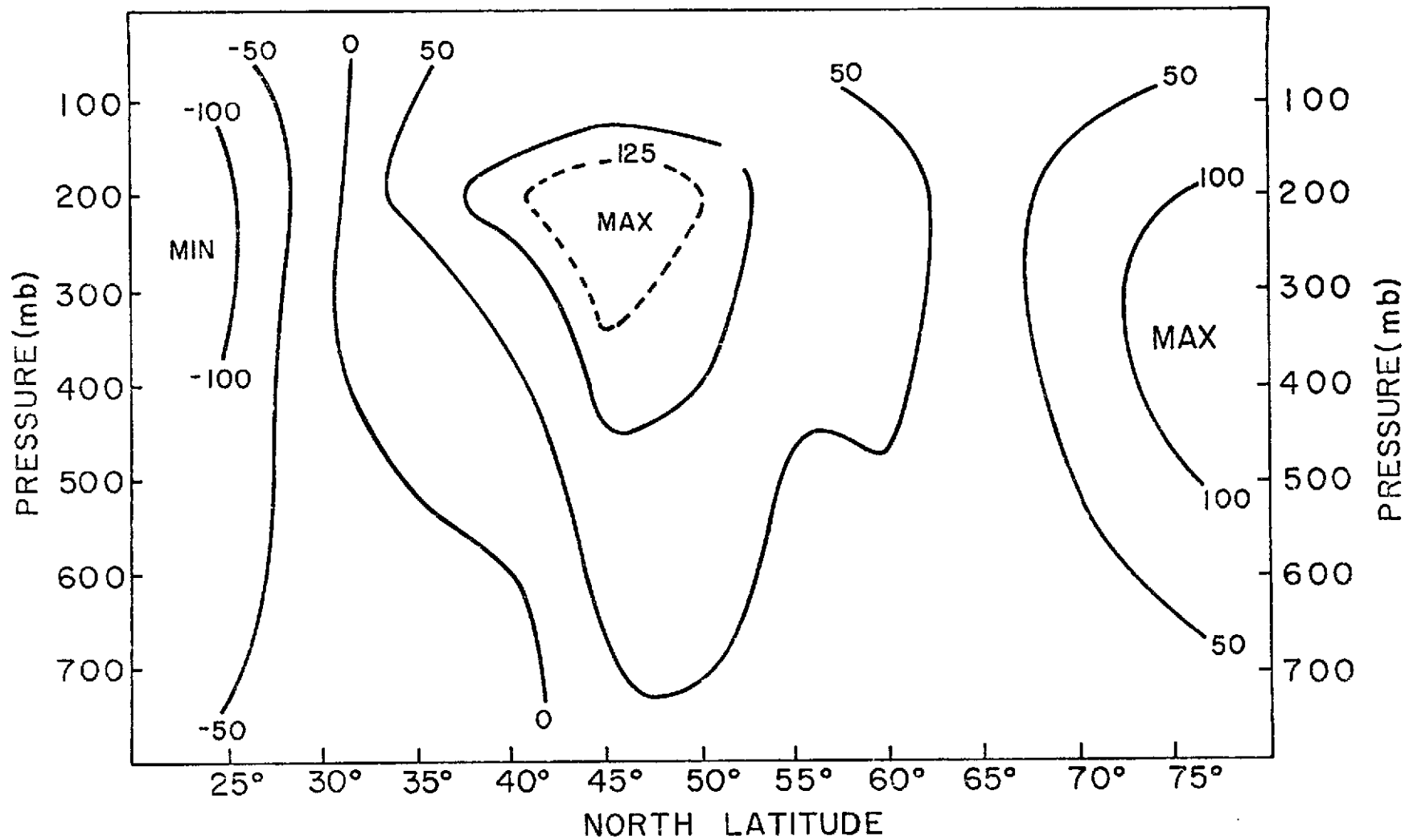
Figure 1d. The distribution of $[\zeta_g]_{(t,\lambda)}$ in April 1970. Units: $10^{-7}s^{-1}$.
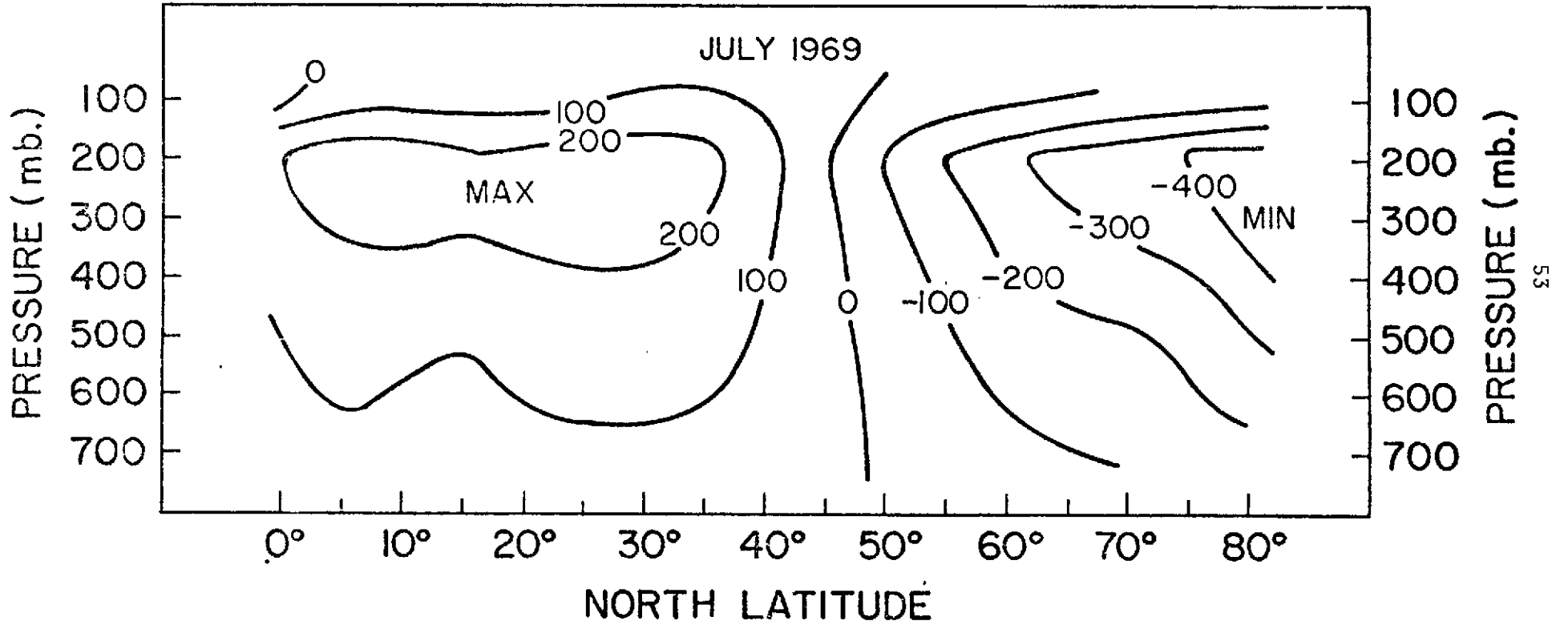
Figure 2a. The distribution of $[H]_{(t,\lambda)} - [H]_{(t,\lambda,\phi)}$ in July 1969. Units: geopotential meters.
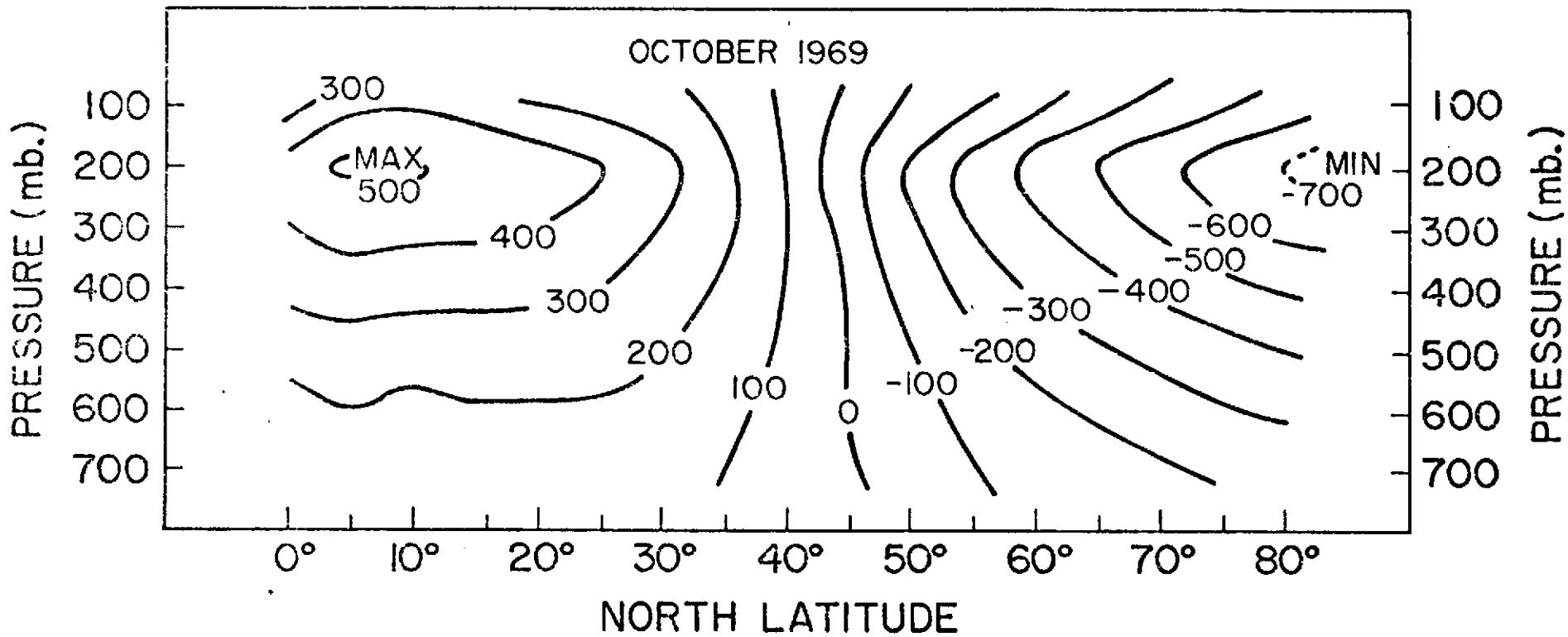
Figure 2b. The distribution of $[H]_{(t,\lambda)} - [H]_{(t,\lambda,\phi)}$ in October 1969. Units: geopotential meters.
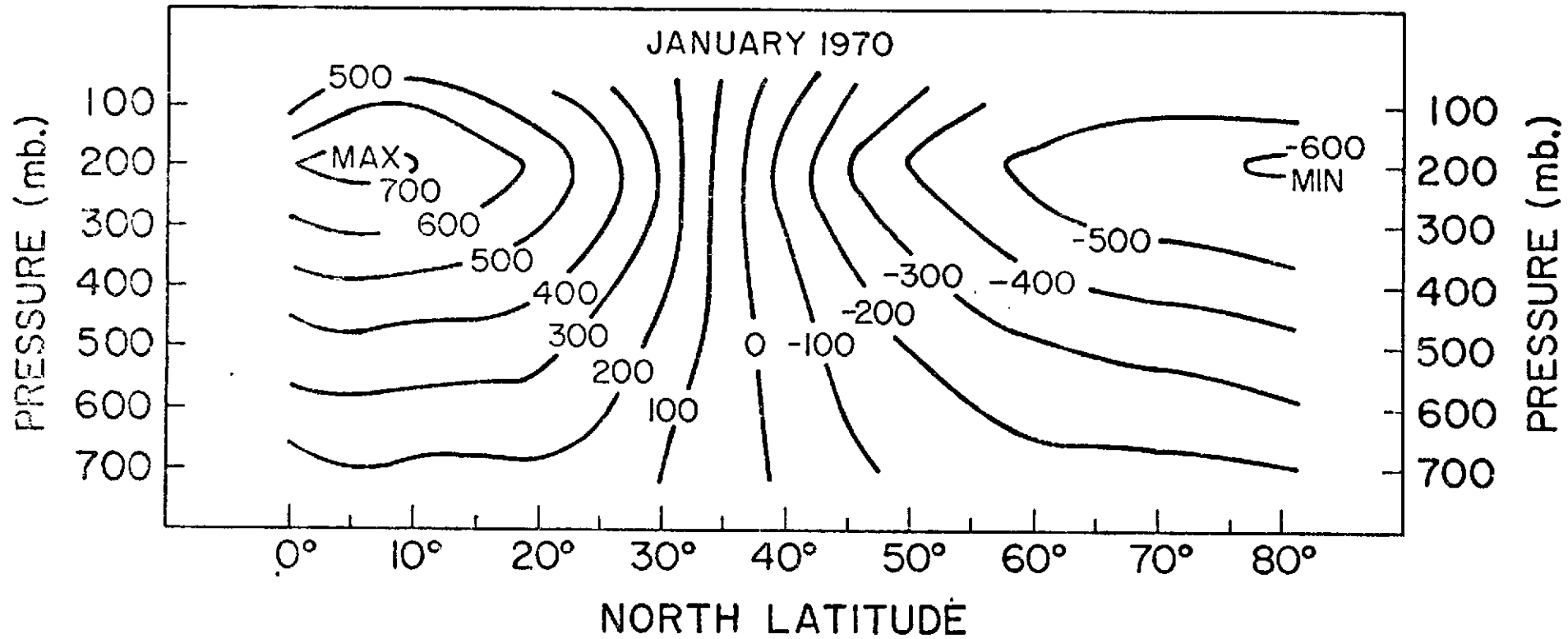
Figure 2c. The distribution of $[H]_{(t,\lambda)} - [H]_{(t,\lambda,\phi)}$ in January 1970. Units: geopotential meters.
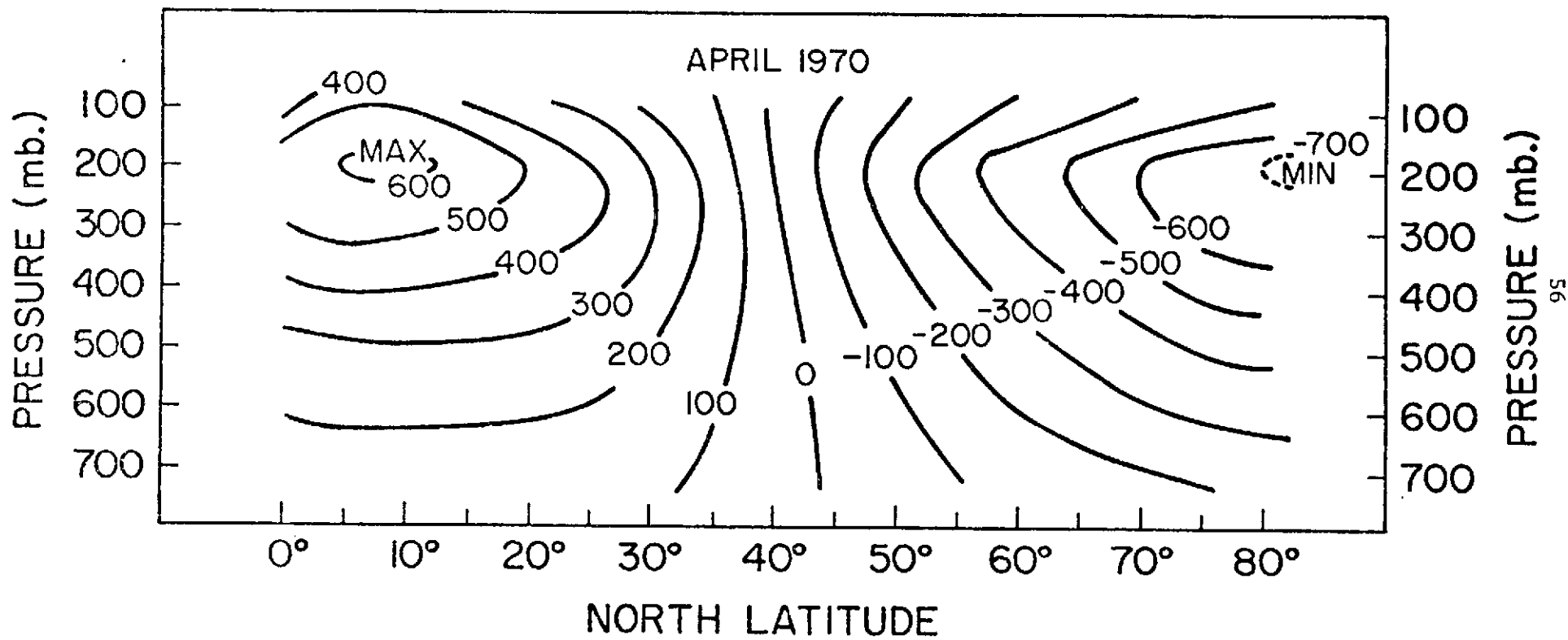
Figure 2d. The distribution of $[H]_{(t,\lambda)} - [H]_{(t,\lambda,\phi)}$ in April 1970. Units: geopotential meters.
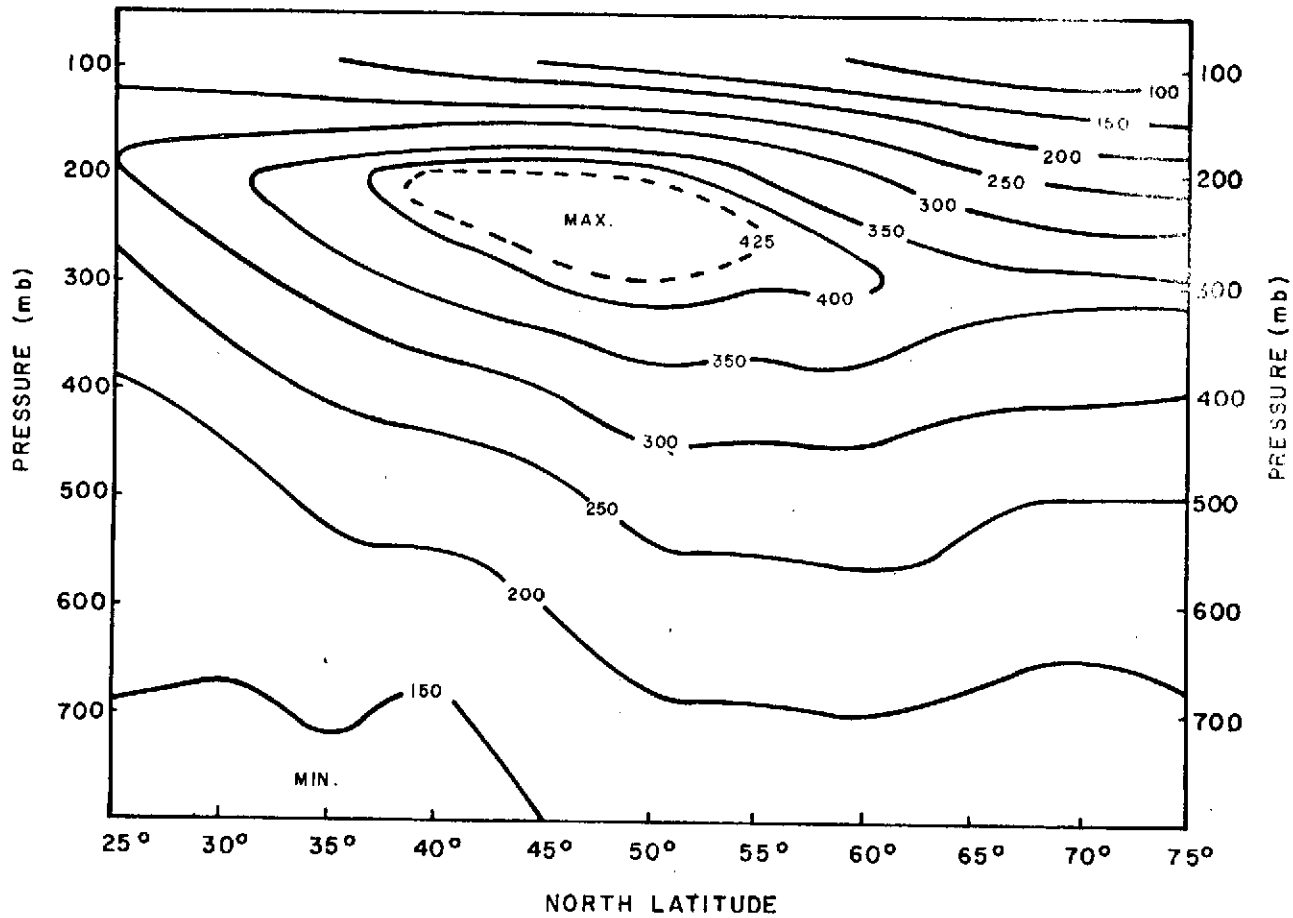
Figure 3a. The distribution of K in July 1969.
Units: $10^{-7}s^{-1}$.
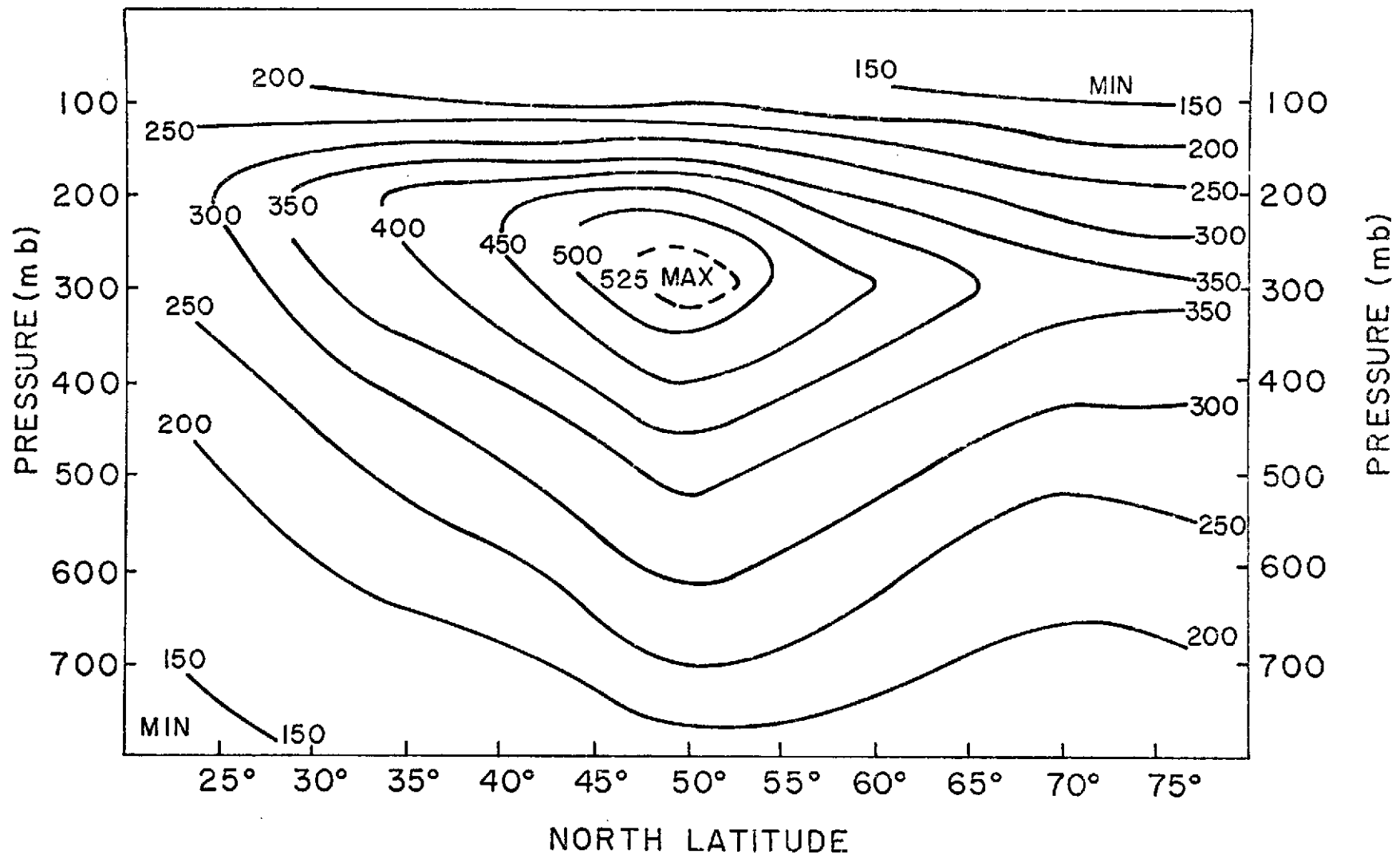
Figure 3b. The distribution of K in October 1969.
Units: $.10^{-7}s^{-1}$.

58
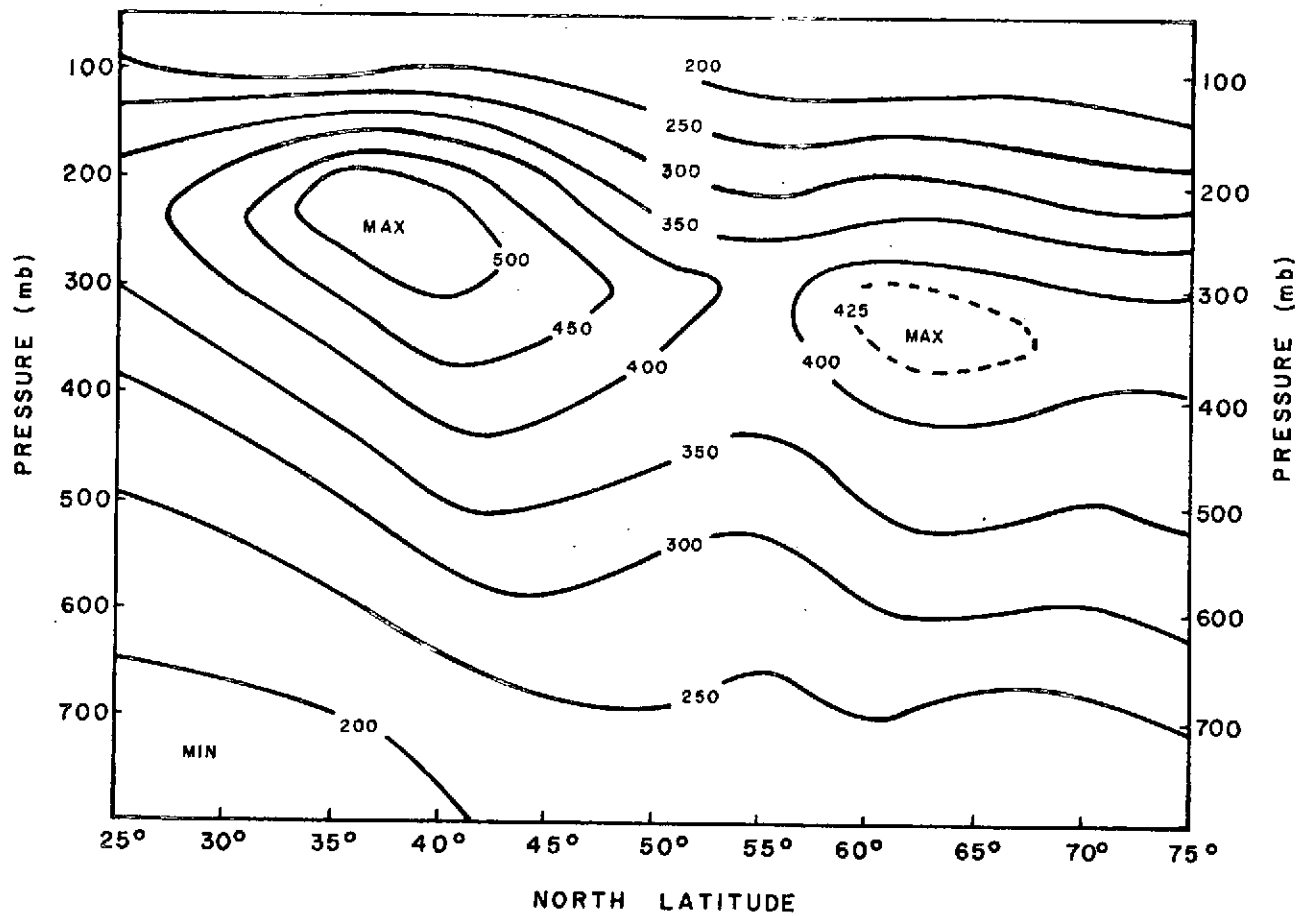
Figure 3c. The distribution of K in January 1970.
Units: $10^{-7}s^{-1}$.
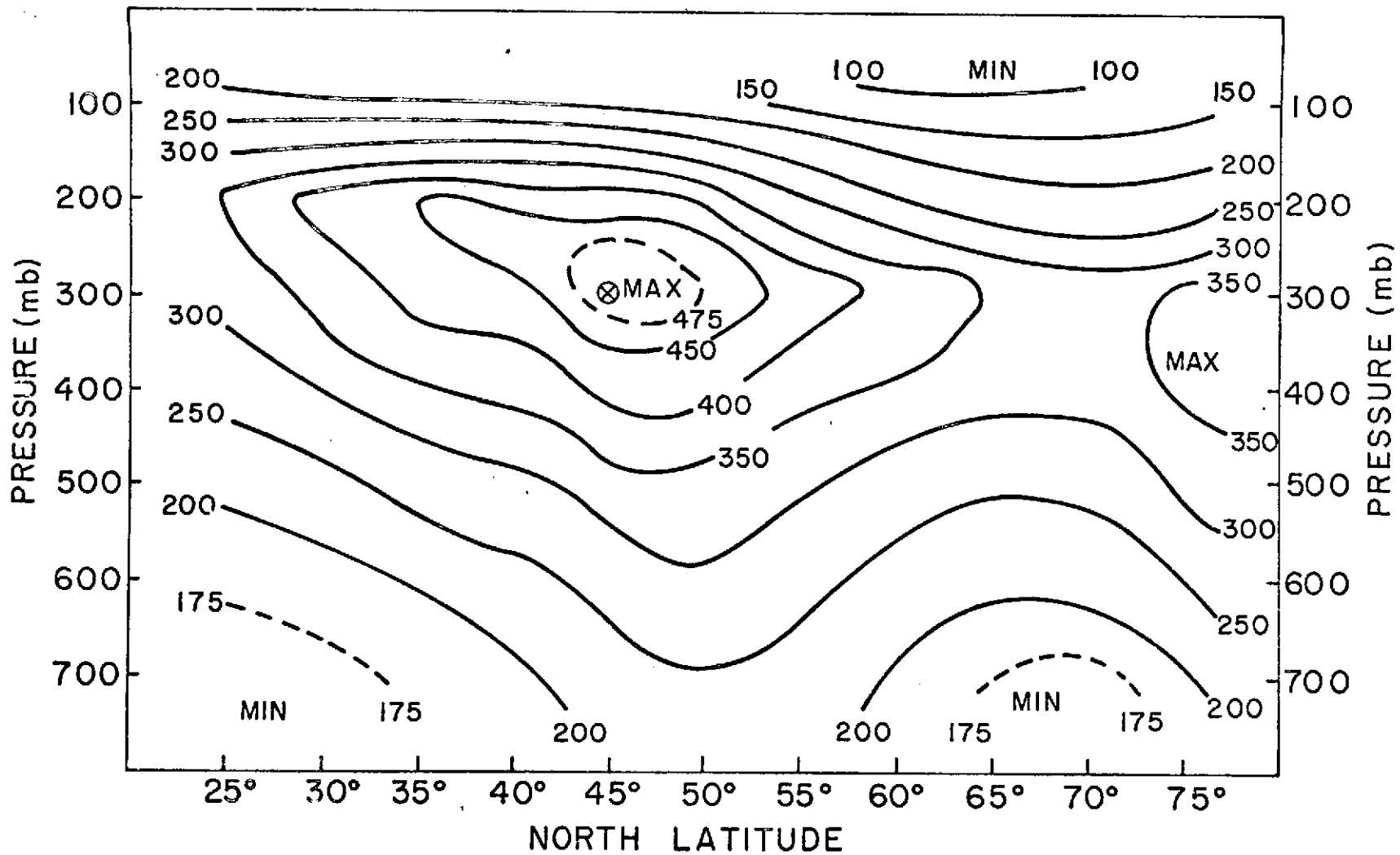
Figure 3d. The distribution of K in April 1970.
Units: $10^{-7}s^{-1}$.
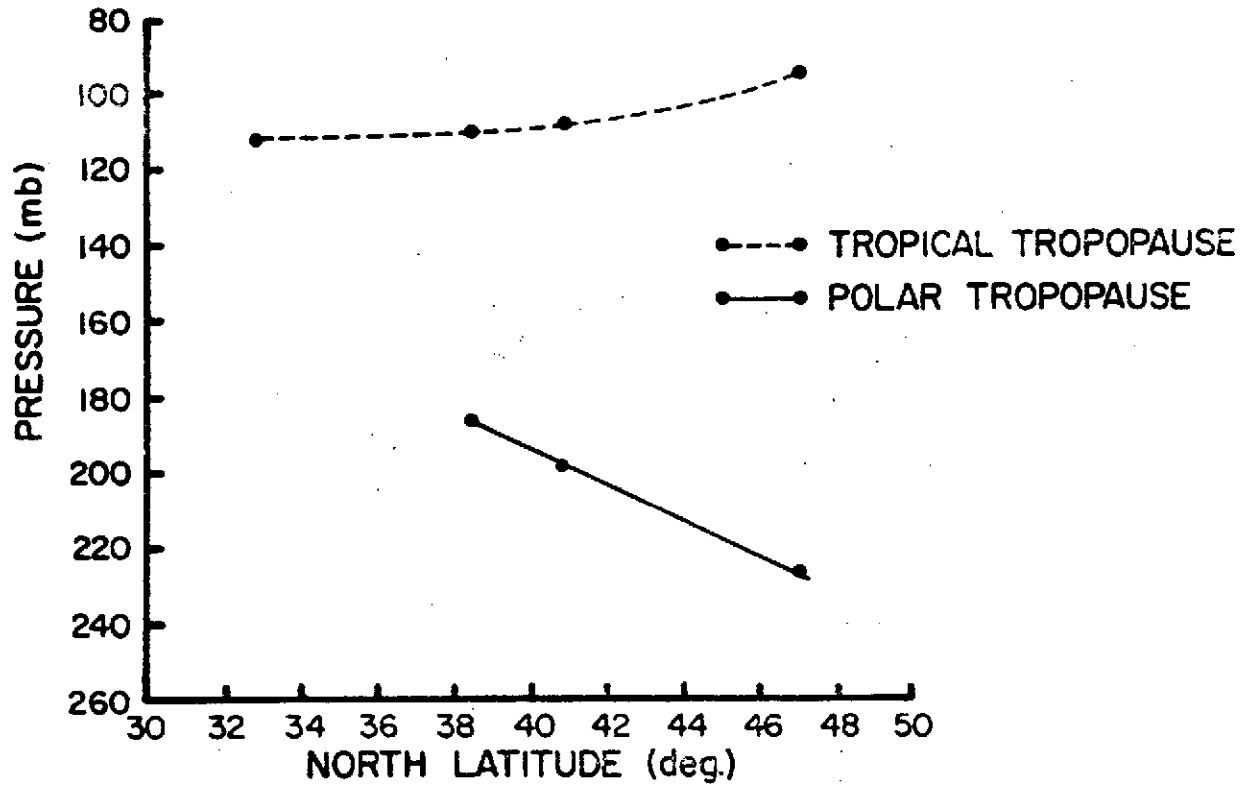
Fig. 3e.- Mean July 1969 tropopauses along North American coastal regions.
A tertiary region of stability exists at about the 140 mb level
at most latitudes considered here.
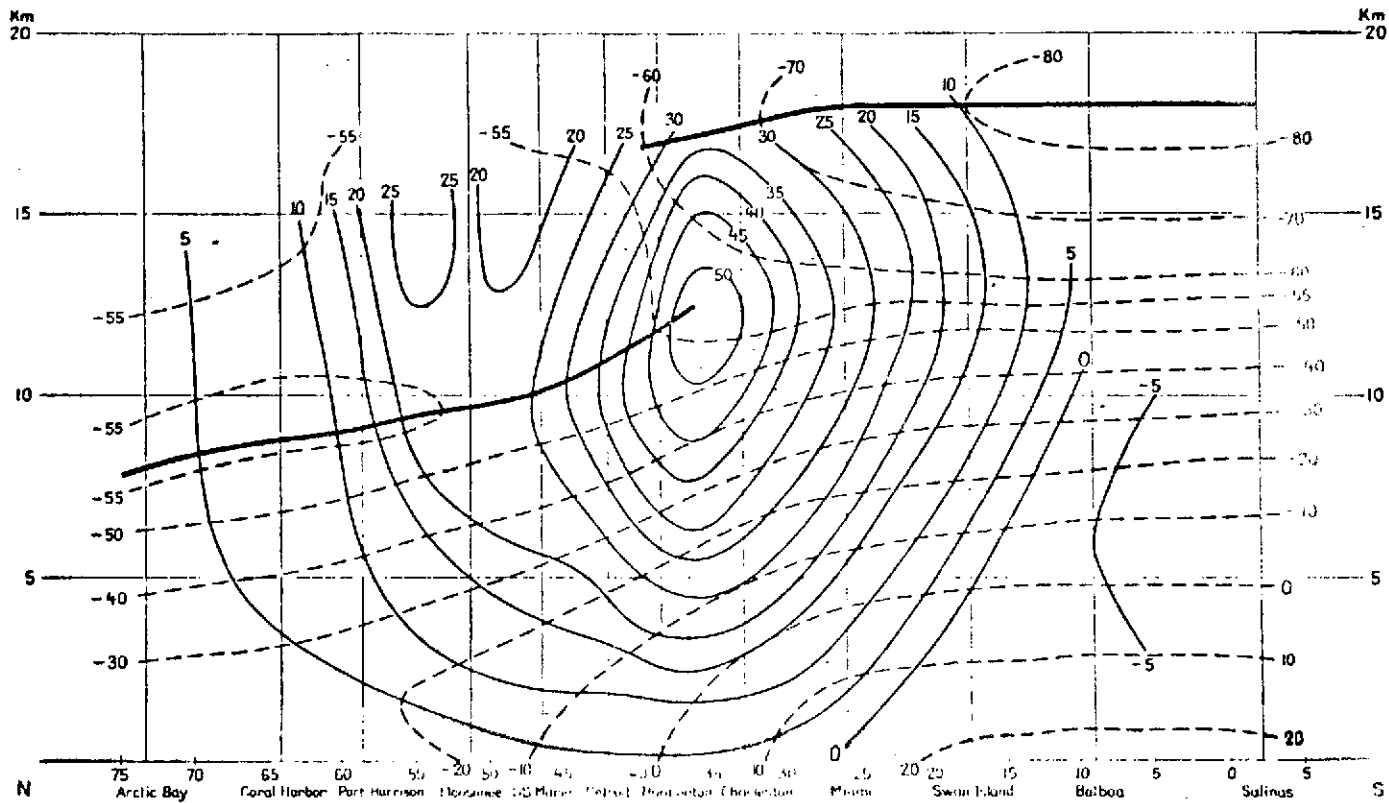
Figure 3f. Observed mean temperatures and mean geostrophic zonal winds, computed from the observed pressure and temperature data in a vertical north-south section through North and Central America. Computed and drawn by Dr. Seymour L. Hess; based on daily radiosonde data for January and February, 1941 through 1945 (winter conditions). (From Rossby (1949).)
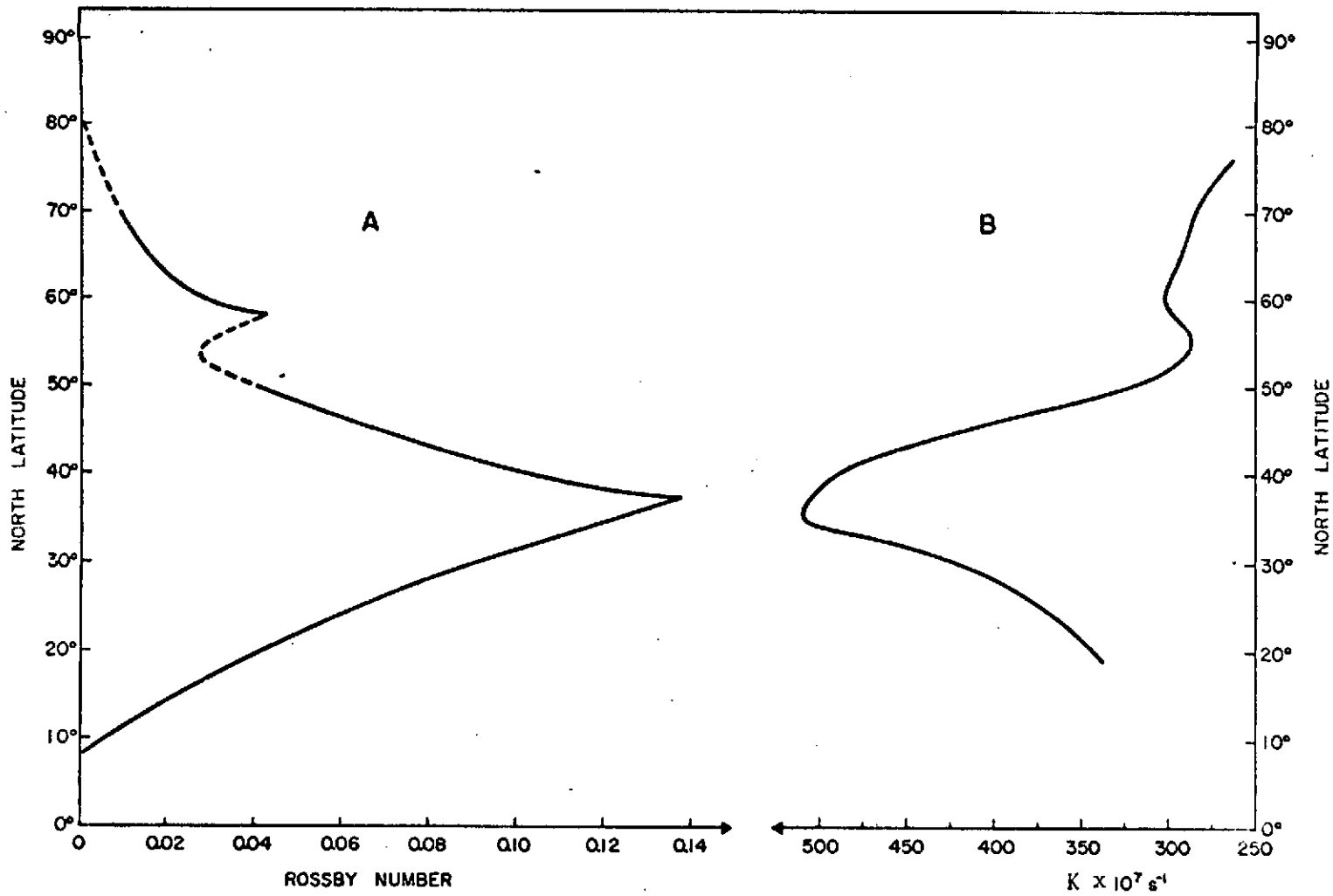
Figure 3g.   Mean zonal-wind profile for 12-km level in winter. The data for this curve are taken from the section in Fig. 10. Note the indications of a second, weaker jet near 55N. (After Rossby (1949)).

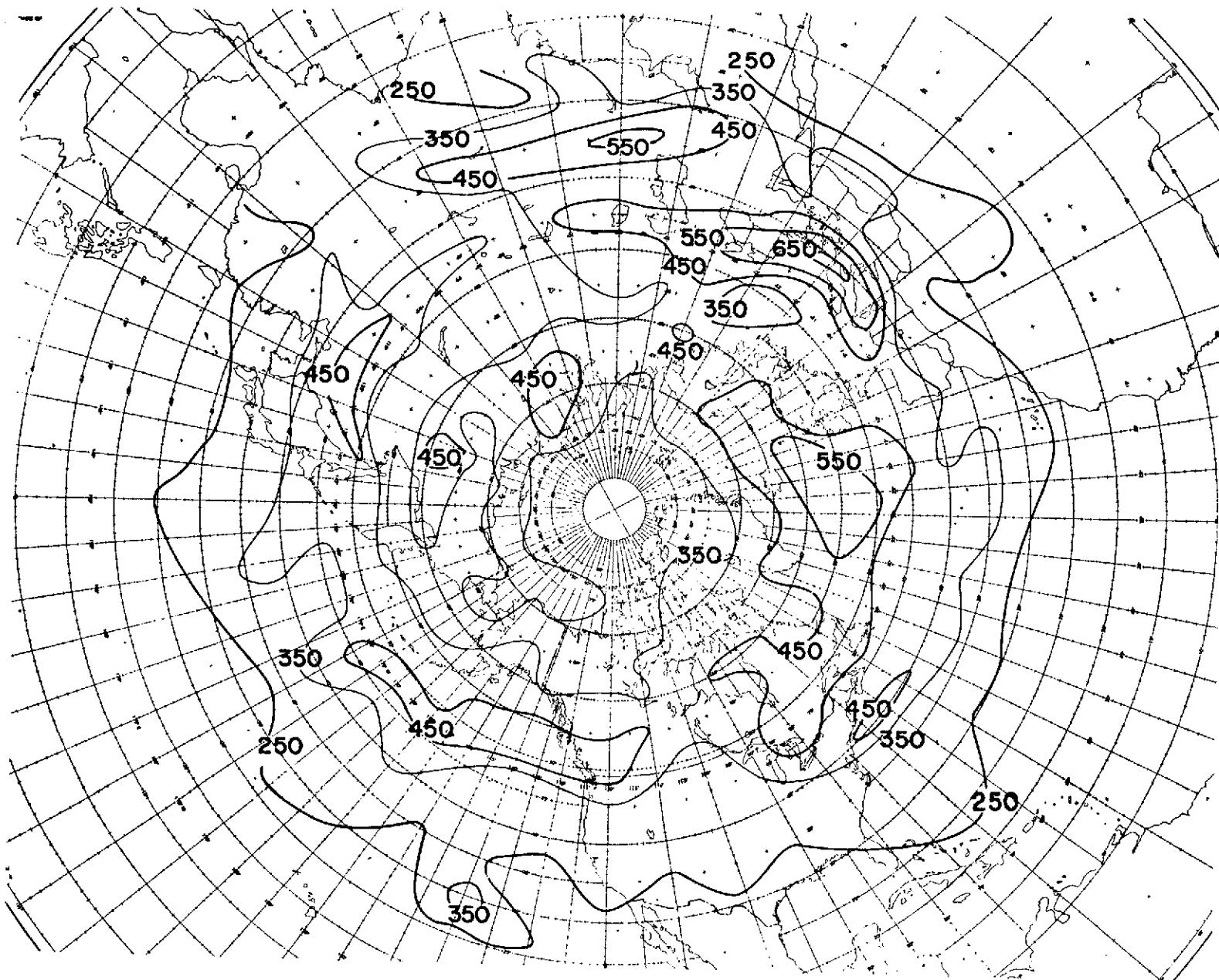Figure 3h.   The parameter K at the 200 mb level in January 1970.
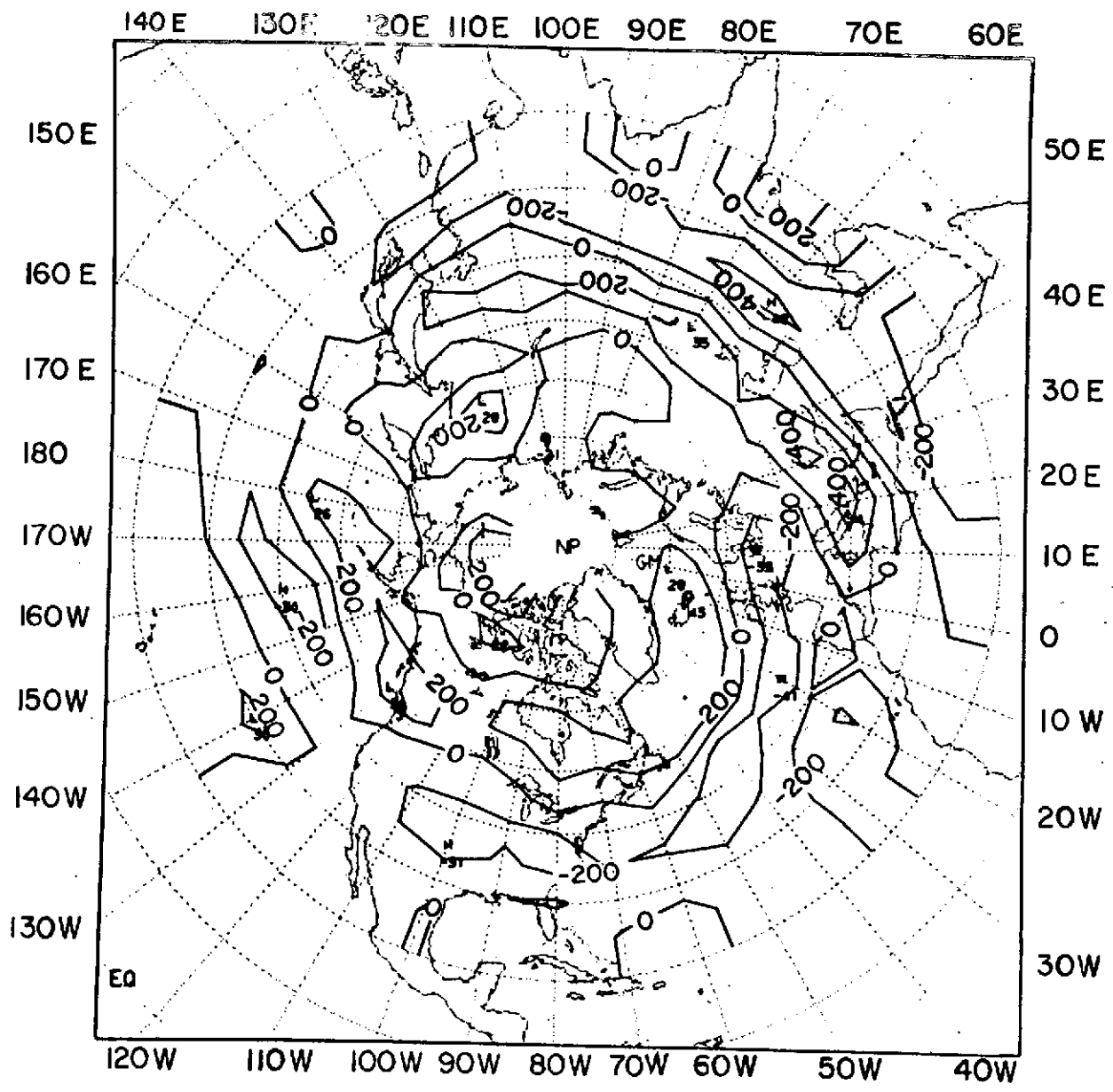
Figure 4a. The geographical distribution of $[\zeta_g]_{(t)}$ in July 1969, at the 300 mb level. Units: $10^{-7}s^{-1}$.
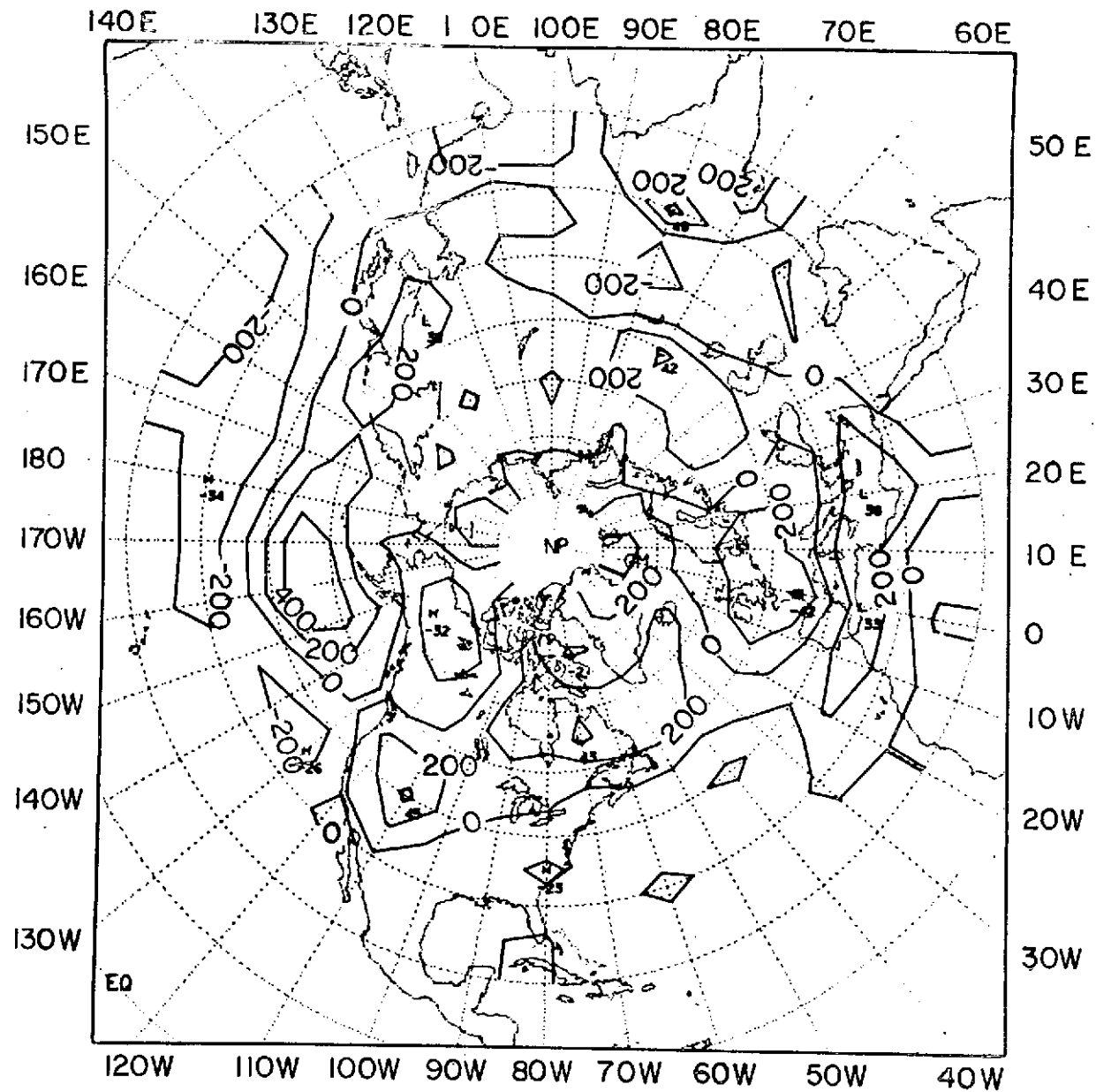
Figure 4b. The geographical distribution of $[\zeta_g]_{(t)}$ in October 1969, at the 300 mb level. Units: $10^{-7} s^{-1}$.
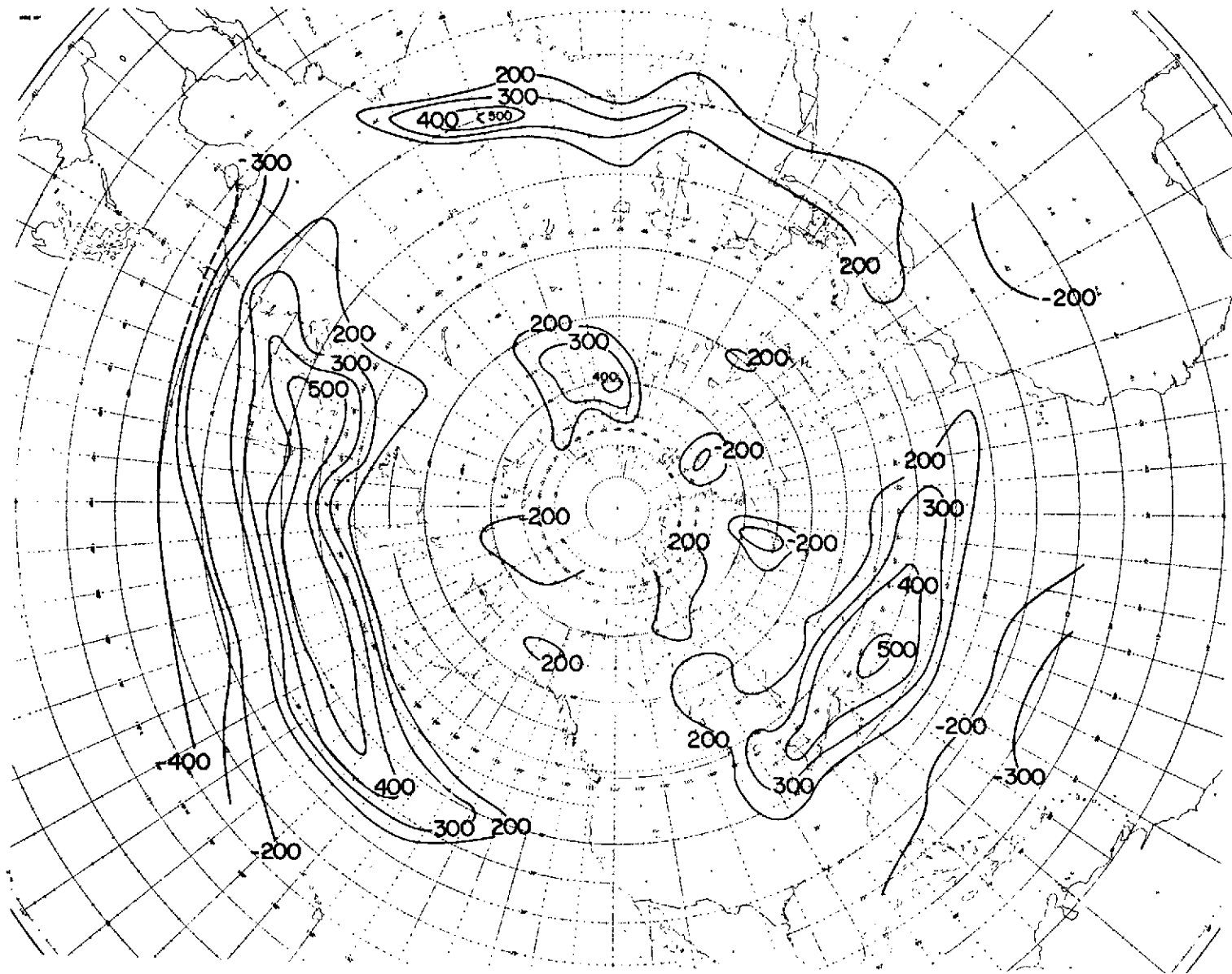
Figure 4c. The geographical distribution of $[\zeta_g]_{(t)}$ in January 1970, at the 300 mb level. Units: $10^{-7}s^{-1}$.
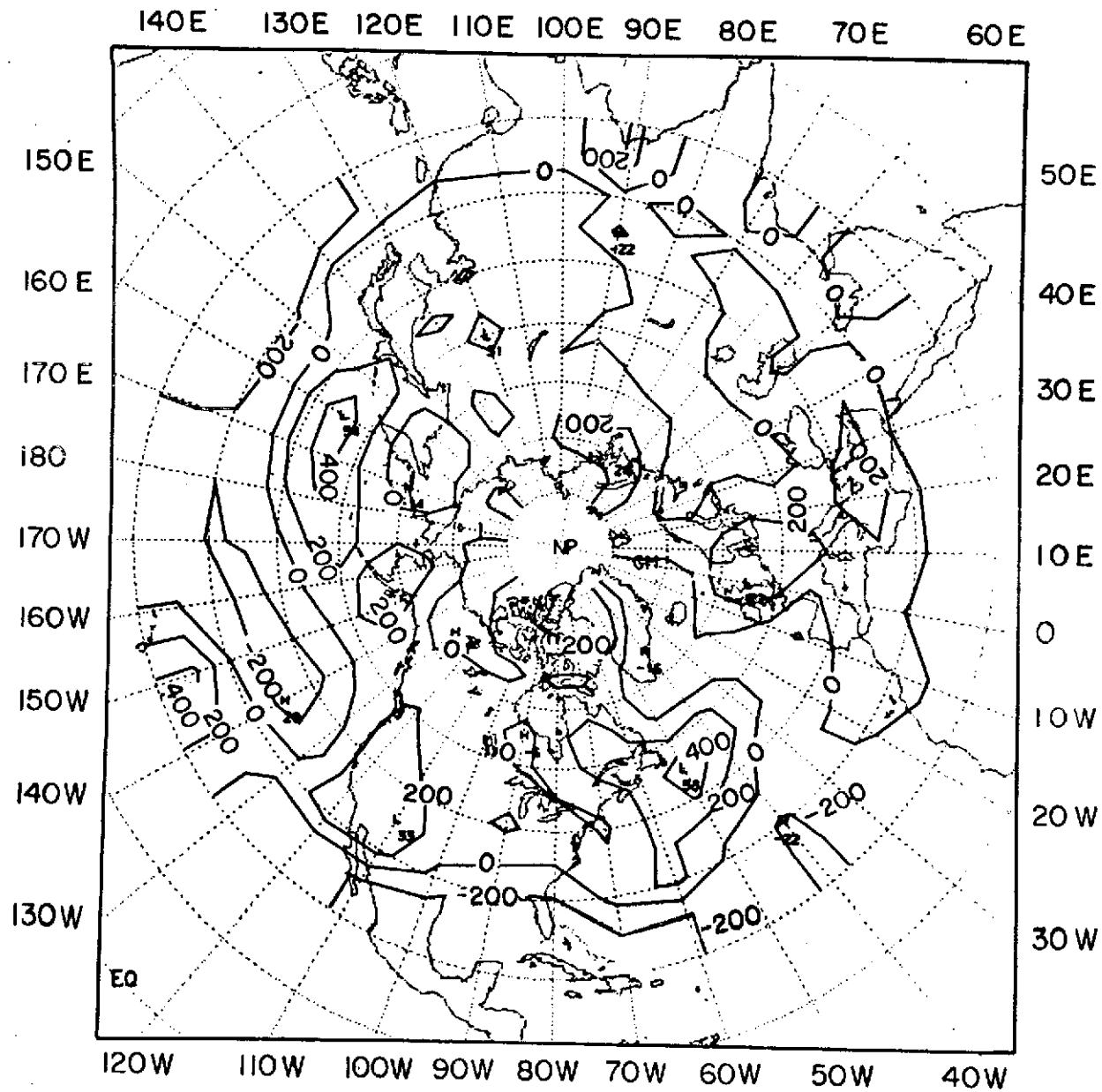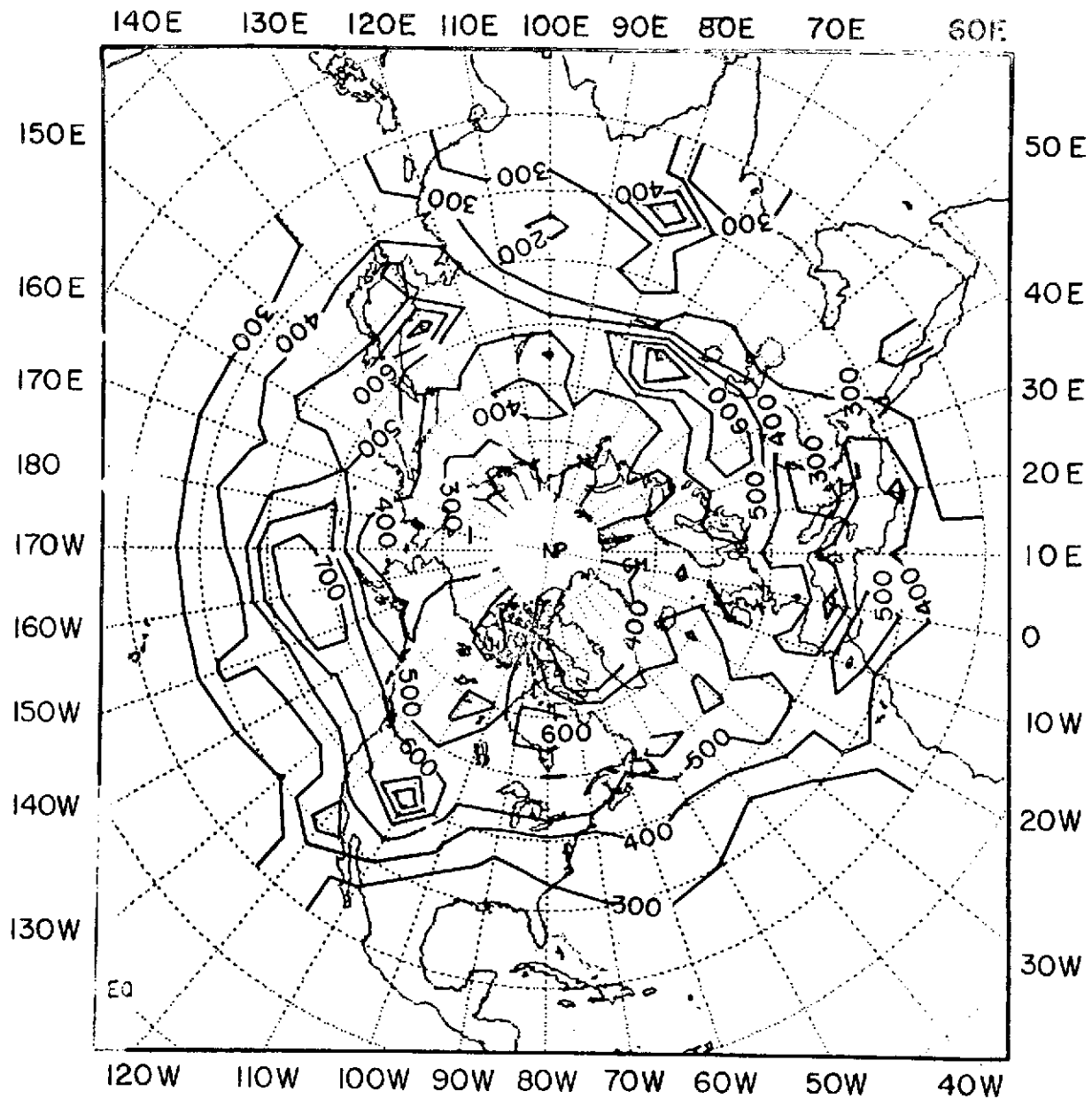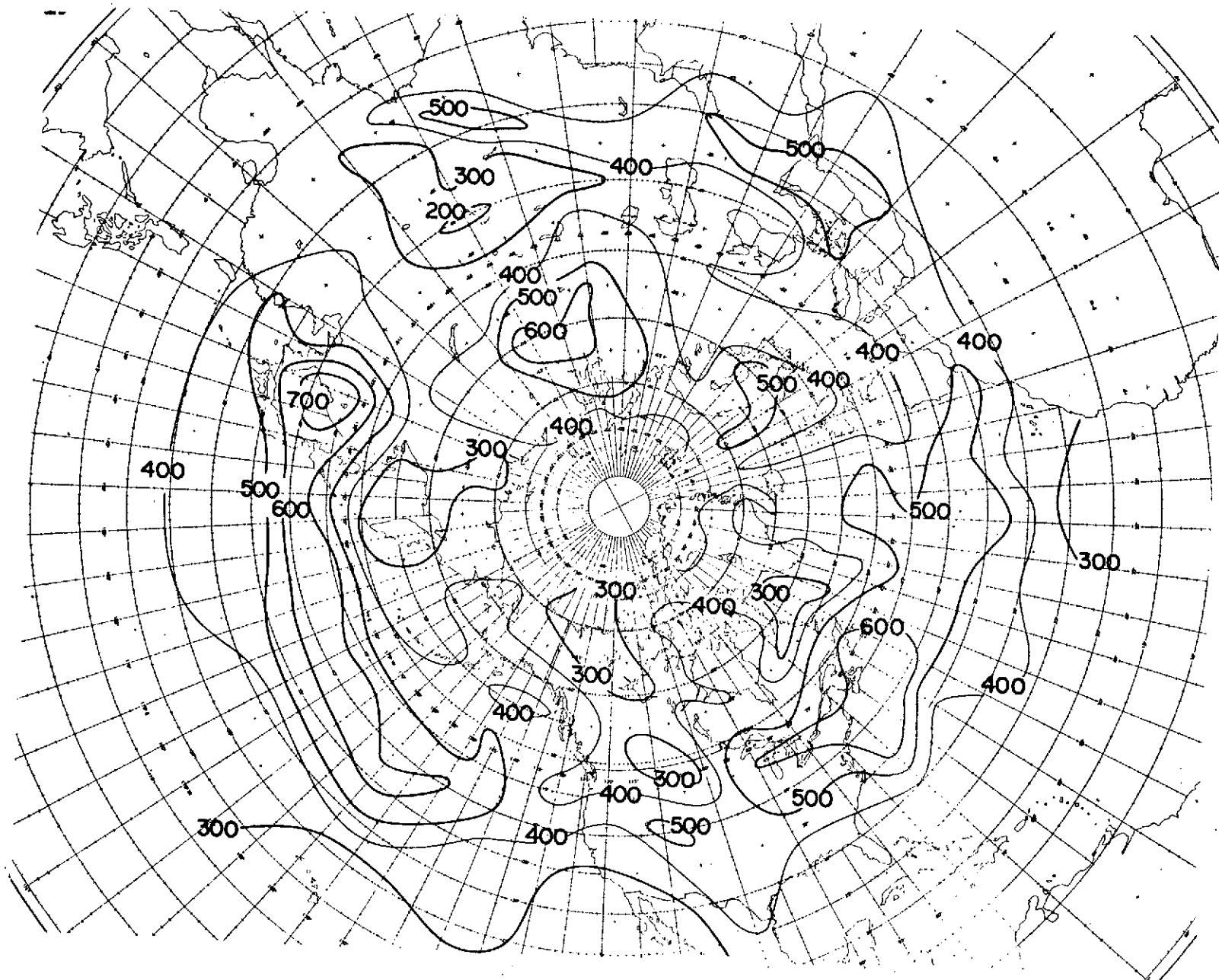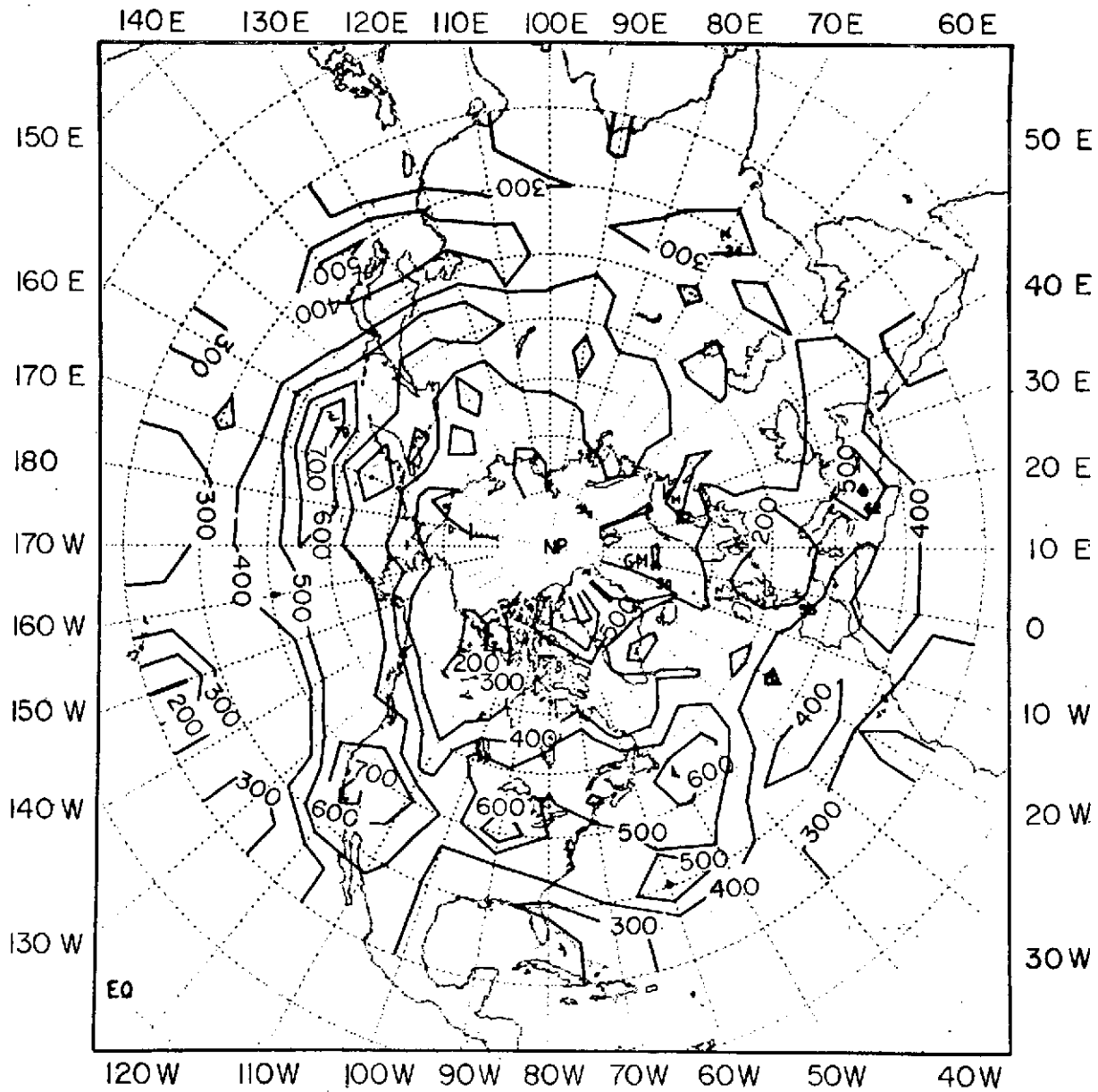
Figure 4d. The geographical distribution of $[\zeta_g]_{(t)}$ in April 1970, at the 300 mb level. Units: $10^{-7}s^{-1}$.

Figure 5a. The geographical distribution of $\{\zeta_g\}_{(t)}$ in July 1969, at the 300 mb level. Units: 10^{-7}s^{-1}.

150 E

160 E

170 E

180

170 W

160 W

150 W

140 W

130 W

50 E

40 E

30 E

20 E

IO E

0

IO W

20 W

30 W

NP

EQ

120W   IIOW   IOOW 90W 80W 70W 60W   50W   40W

Figure 5b.   The geographical distribution of $\{\zeta_g\}_{(t)}$ in
October 1969, at the 300 mb level. Units:
$\sim 10^{-7}\mathrm{s}^{-1}$.

Figure 5c. The geographical distribution of $\{\zeta_g\}_{(t)}$ in January 1970, at the 300 mb level. Units: $10^{-7}s^{-1}$.

Figure 5d. The geographical distribution of $\{\zeta_g\}_{(t)}$ in
April 1970, at the 300 mb level. Units:
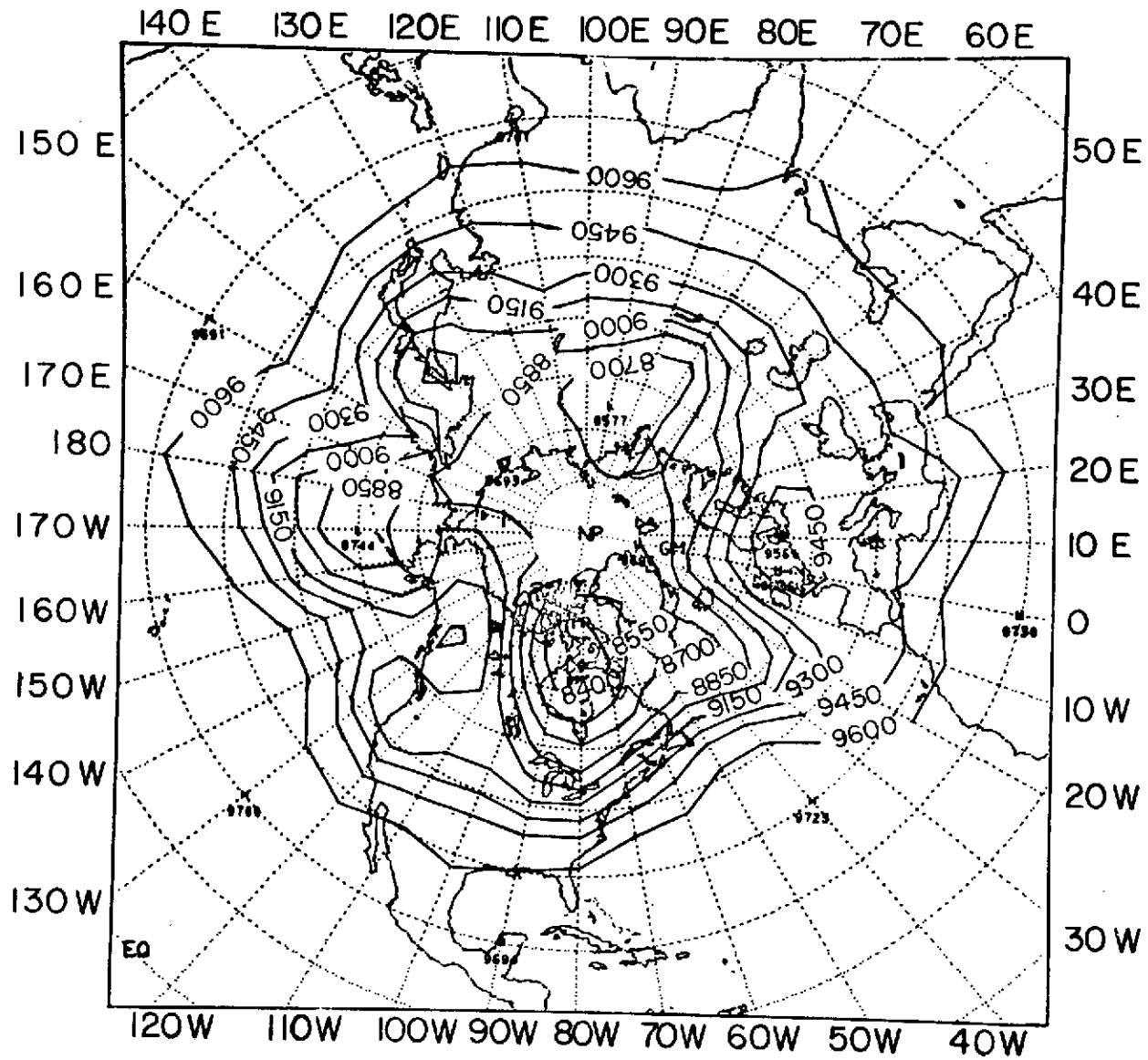$10^{-7}s^{-1}$.

Figure 6. The geopotential height distribution at the 300 mb level on October 17, 1970. Units: geopotential meters.
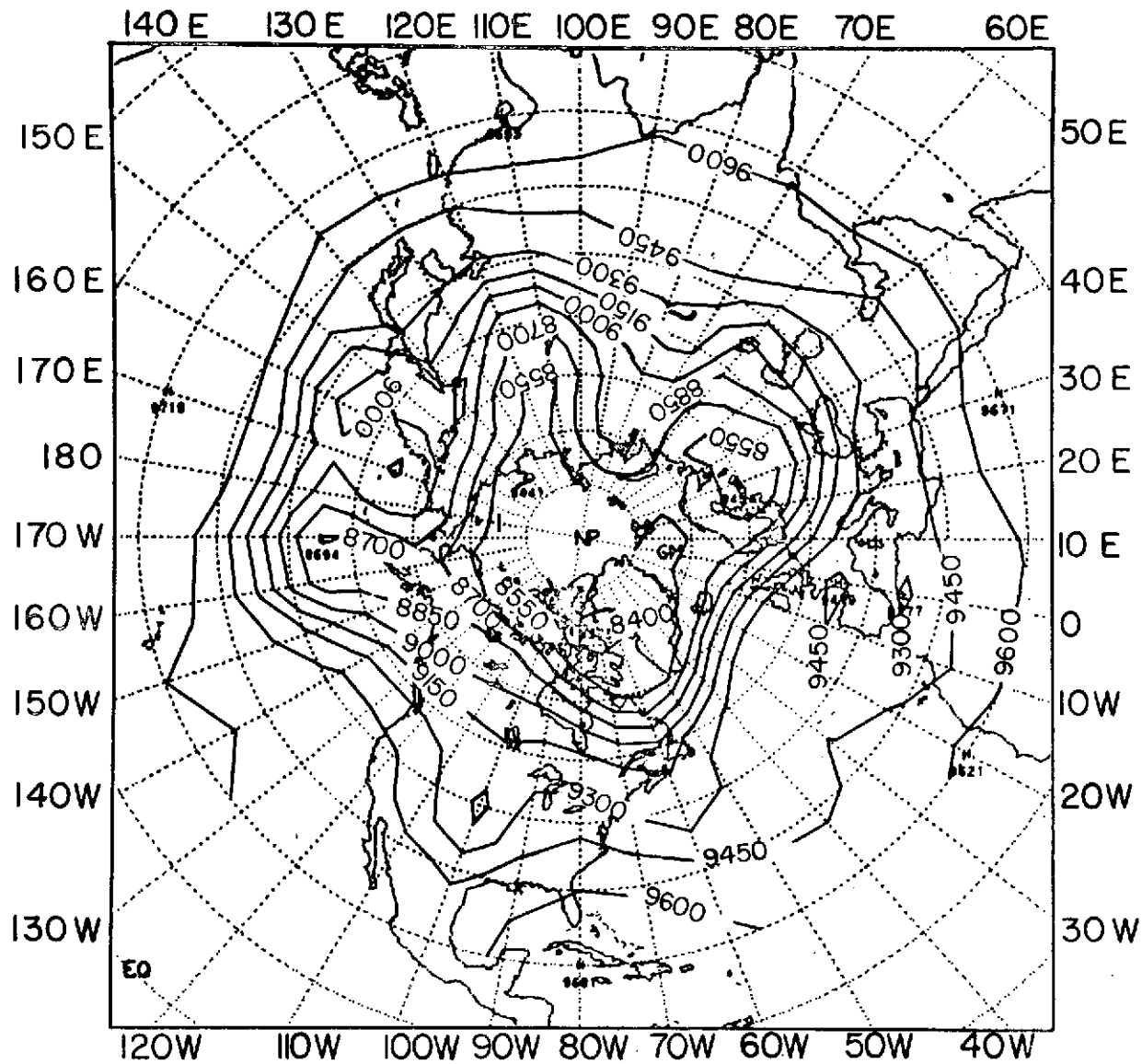
Figure 7. The geopotential height distribution at the 300 mb
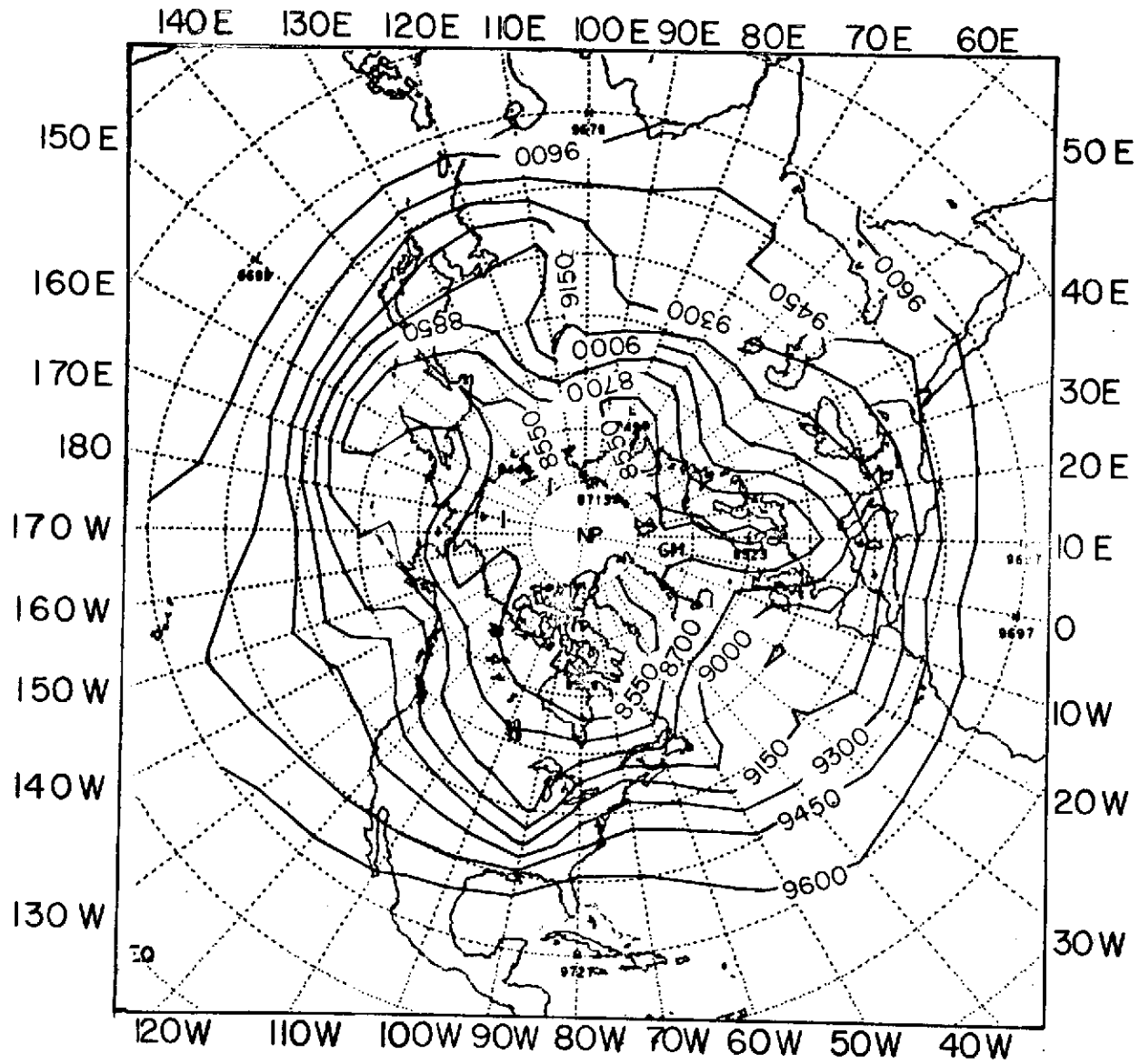level on October 30, 1970. Units: geopotential
meters.

Figure 8. The geopotential height distribution at the 300 mb level on April 2, 1970. Units: geopotential meters.